Table II. *Univariate and multivariate analysis for overall survival (Cox proportional hazards regression model).*

	Univariate analysis			Multivariate analysis		
Factors	RR	95% CI	*p*-Value	RR	95% CI	*p*-Value
Tumor size (<30mm/30mm <)	2.11	1.15-5.28	0.01*	1.06	0.51-2.77	0.88
Serosal invasion (absent/present)	2.05	1.39-3.11	<0.001*	1.36	0.87-2.19	0.17
Lymphatic invasion (absent/present)	1.67	1.13-2.52	0.009*	1.05	0.65-1.72	0.82
Venous invasion (absent/present)	2.08	1.40-3.07	<0.001*	1.71	1.07-2.75	0.02*
Liver metastasis (absent/present)	3.75	2.42-5.61	<0.001*	2.94	1.69-5.12	<0.001*
Peritoneal metastasis (absent/present)	5.61	2.37-13.29	<0.001*	7.16	1.40-14.50	0.01*
Lymph node metastasis (absent/present)	2.22	1.45-3.68	<0.001*	1.26	0.74-2.25	0.39
HMGB1 expression (low/high)	1.66	1.11-2.60	0.01*	1.59	1.00-2.65	0.04*

RR, Rerative risk; CI, confidence interval; *$p<0.05$.

Statistical analysis. Data from qRT-PCR analyses were analyzed using the JMP 5 software (JMP, Cary, NC, USA). The relationships between *HMGB1* expression and clinicopathological factors were analyzed using the Student's *t*-tests, Chi-squared tests and analysis of variance (ANOVA). Overall survival (OS) curves were plotted using the Kaplan-Meier method measured from the day of surgery, while the log-rank test was applied for comparisons. All differences were statistically significant at the level of $p<0.05$. The relative multivariate significance of potential prognostic variables was also examined. The Cox proportional hazards regression was used to test the independent prognostic contribution of *HMGB1*.

Results

HMGB1 mRNA expression in 140 tumor tissues from CRC patients was examined by qRT-PCR to investigate the clinical significance of *HMGB1* in CRC. As a control, we measured *HMGB1* mRNA expression in normal tissues from the same patients. *HMGB1* expression was significantly higher in tumor than in normal tissues (Figure 1A). Additionally, we divided the 140 patients with CRC into a high-*HMGB1*-expression group (n=70) and a low-HMGB1-expression group (n=70) according to the median expression level in tumor tissues and analyzed clinicopathological factors in the high and low *HMGB1* mRNA expression groups (Table I). The high-*HMGB1*-expression group showed greater lymphatic invasion and lymph node metastasis than the low-*HMGB1*-expression group. Furthermore, the high-*HMGB1*-expression group exhibited significantly larger tumors than the low-*HMGB1*-expression group. With regard to OS, patients with high *HMGB1* expression had significantly poorer prognoses than those with low *HMGB1* expression ($p=0.0051$) (Figure 1B). Univariate and multivariate analyses showed that *HMGB1* mRNA expression was an independent prognostic indicator of OS in patients with CRC (relative risk, 1.59; $p=0.04$) (Table II).

To clarify the correlation of HMGB1 expression with CRC, HMGB1 protein levels were investigated in colon cancer tissues and lymph node metastases by immunohistochemical analysis. As shown in Figures 2 and 3, HMGB1 protein was highly expressed in cancer cells from both CRC tissues and corresponding metastatic lymph node tissues, suggesting that colon cancer cells expressing HMGB1 might lead to lymph node metastasis. Furthermore, high HMGB1 expression was present in the cytoplasm and nucleus of primary tumor tissues in case 1, while high HMGB1 expression was only in the cytoplasm in case 2.

Discussion

Our study revealed that *HMGB1* mRNA expression was significantly higher in CRC tissues than in noncancerous tissues. Several previous studies have supported the significance of HMGB1 in CRC, demonstrating that HMGB1 is overexpressed in CRC tissues. Xiang *et al*. first reported that colorectal adenocarcinoma tissues contain higher HMGB1 levels than corresponding noncancerous mucosa, as analyzed by tissue microarray (19). Moreover, elevated *HMGB1* mRNA levels have been detected in 40% of all colon carcinomas by using microarray analyses to establish expression profiles (18). In the current study, we presented definitive findings of *HMBG1* expression in CRC tissues and regional lymph node metastases using a much larger sample size than those described in previous reports.

Our study also, firstly, showed that *HMGB1* mRNA expression in CRC tissues was related to a poor prognosis and that high expression of *HMGB1* mRNA in CRC tissues was significantly associated with tumor volume, lymphatic invasion and lymph node metastasis. These data indicated that HMGB1 induced the progression, invasion and migration of cancer cells. To explore whether HMGB1 may be involved in lymphatic invasion and lymph node metastasis, we investigated the expression of HMGB1 in tumor tissues derived from primary tumors and lymph nodes by immunohistochemical analysis. We demonstrated that the

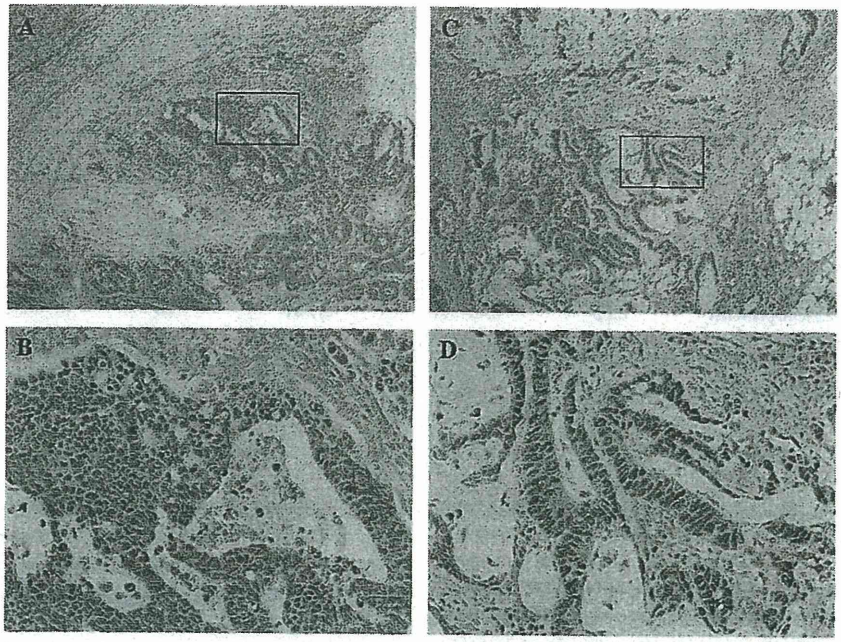

Figure 2. *Immunohistochemical staining in human clinical samples of CRC tissues and the corresponding lymph node metastasis tissues in case 1. (A) High expression of HMGB1 in both cytoplasm and nucleus of cancer cells in CRC tissues (original magnification ×40); (B) Larger magnifications (×200) of boxed region in (A); (C) High expression of HMGB1 in both cytoplasm and nucleus of cancer cells in the corresponding lymph node metastasis tissues (original magnification ×40); (D) Larger magnifications (×200) of boxed region in (C).*

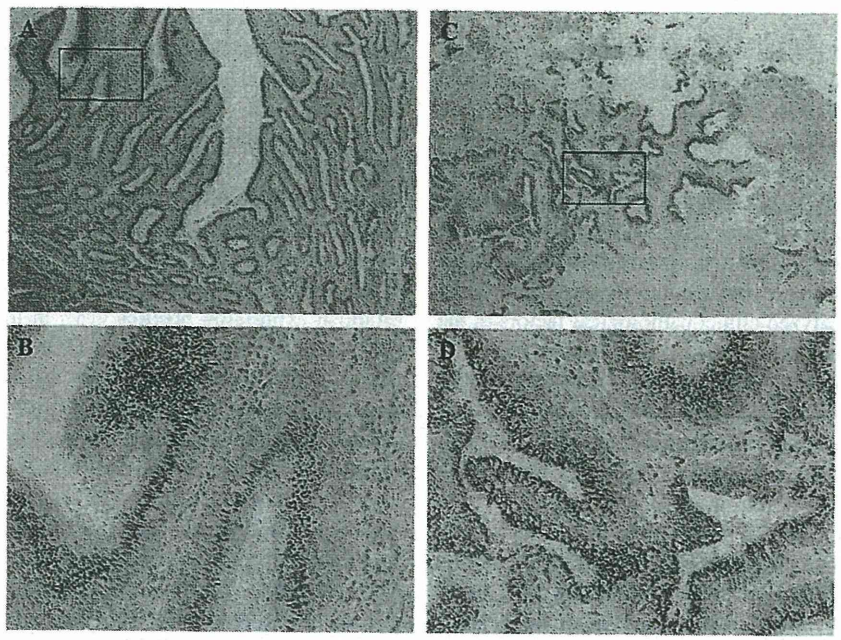

Figure 3. *Immunohistochemical staining in human clinical samples of CRC tissues and the corresponding lymph node metastasis tissues in case 2. (A) High expression of HMGB1 only in the cytoplasm of cancer cells in CRC tissues (original magnification ×40); (B) Larger magnifications (×200) of boxed region in (A); (C) High expression of HMGB1 only in the cytoplasm of cancer cells in the corresponding lymph node metastasis tissues (original magnification ×40); (D) Larger magnifications (×200) of boxed region in (C).*

level of HMGB1 expression in lymph node metastases was equivalent to that of corresponding primary tumors.

Moreover, our immunohistochemical analysis revealed that 20% of malignant cells expressed the HMGB1 protein in both the cytoplasm and nucleus; however, the remaining cancer cells showed HMGB1 expression only in the cytoplasm. In previous studies, HMGB1 has been shown to act as a tumor-promoting factor, performing multiple functions. Inside the cell, HMGB1 is a highly conserved chromosomal protein that acts as a DNA chaperone that has been known to enhance the activity of ftranscriptional activators and repressors by binding to transcription factors (20, 21). HMGB1 is also released into the extracellular space, where it binds to cell surface receptors, such as receptor for advanced glycation end-products [RAGE] and Toll-like receptor 4 [TLR4], to activate the downstream signaling pathways (nuclear factor κB [NF-κB], mitogen-activated protein kinase [MAPK] and phosphoinositol 3 kinase [PI3K]). Activation of these downstream pathways produces a functional response, leading to activation of cell adhesion and migration, promotion of cell proliferation and induction of angiogenesis (22-24). These previous studies support that HMGB1 protein exists in both the cytoplasm and nucleus of cancer cells, consistent with the results of our immunocytochemical analysis.

As described above, the expression of HMGB1 was correlated with various clinicopathological factors and could be a critical indicator of tumor aggressiveness and metastasis in primary CRC. In particular, it is possible that lymph node metastasis could be predicted from the *HMBG1* gene expression levels, as determined from small-biopsy samples. However, the function of HMGB1 has not been clearly elucidated and further studies are needed to determine the mechanisms through which HMGB1 exerts its tumor-promoting effects in CRC.

In conclusion, we demonstrated that HMGB1 is a powerful prognostic marker in CRC and involved in mediating lymphatic invasion and lymph node metastasis. Our data suggest that investigation of HMGB1 expression in CRC tissues may help physicians to predict lymph node metastasis and clinical prognosis.

Conflicts of Interest

The Authors declare no conflicts of interest.

Acknowledgements

We thank K. Oda, M. Kasagi and S. Kono for their technical assistance. This work was supported in part by the following grants and foundations: CREST, Japan Science and Technology Agency (JST); and the Funding Program for Next Generation World-Leading Researchers (LS094).

References

1 Bustin M, Lehn DA and Landsman D: Structural features of the HMG chromosomal proteins and their genes. Biochim Biophys Acta *1049*: 231-243, 1990.

2 Scaffidi P, Misteli T and Bianchi ME: Release of chromatin protein HMGB1 by necrotic cells triggers inflammation. Nature *418*: 191-195, 2002.

3 Chen G, Li J, Ochani M, Rendon-Mitchell B, Qiang X, Susarla S, Ulloa L, Yang H, Fan S, Goyert SM, Wang P, Tracey KJ, Sama AE and Wang H: Bacterial endotoxin stimulates macrophages to release HMGB1 partly through CD14- and TNF-dependent mechanisms. J Leukoc Biol *76*: 994-1001, 2004.

4 Wang H, Vishnubhakat JM, Bloom O, Zhang M, Ombrellino M, Sama A and Tracey KJ: Proinflammatory cytokines (tumor necrosis factor and interleukin 1) stimulate release of high mobility group protein-1 by pituicytes. Surgery *126*: 389-392, 1999.

5 Wang H, Bloom O, Zhang M, Vishnubhakat JM, Ombrellino M, Che J, Frazier A, Yang H, Ivanova S, Borovikova L, Manogue KR, Faist E, Abraham E, Andersson J, Andersson U, Molina PE, Abumrad NN, Sama A and Tracey KJ: HMG-1 as a late mediator of endotoxin lethality in mice. Science *285*: 248-251, 1999.

6 Ostberg T, Kawane K, Nagata S, Yang H, Chavan S, Klevenvall L, Bianchi ME, Harris HE, Andersson U and Palmblad K: Protective targeting of high mobility group box chromosomal protein 1 in a spontaneous arthritis model. Arthritis Rheum *62*: 2963-2972, 2010.

7 Park S, Yoon SJ, Tae HJ and Shim CY: RAGE and cardiovascular disease. Front Biosci (Landmark Ed) *16*: 486-497, 2011.

8 Yang H and Tracey KJ: Targeting HMGB1 in inflammation. Biochim Biophys Acta *1799*: 149-156, 2010.

9 Evankovich J, Cho SW, Zhang R, Cardinal J, Dhupar R, Zhang L, Klune JR, Zlotnicki J, Billiar T and Tsung A: High mobility group box 1 release from hepatocytes during ischemia and reperfusion injury is mediated by decreased histone deacetylase activity. J Biol Chem *285*: 39888-39897, 2010.

10 Tang D, Kang R, Cao L, Zhang G, Yu Y, Xiao W, Wang H and Xiao X: A pilot study to detect high mobility group box 1 and heat shock protein 72 in cerebrospinal fluid of pediatric patients with meningitis. Crit Care Med *36*: 291-295, 2008.

11 Huang W, Tang Y and Li L: HMGB1, a potent proinflammatory cytokine in sepsis. Cytokine *51*: 119-126, 2010.

12 Campana L, Bosurgi L and Rovere-Querini P: HMGB1: a two-headed signal regulating tumor progression and immunity. Curr Opin Immunol *20*: 518-523, 2008.

13 Chen J, Xi B, Zhao Y, Yu Y, Zhang J and Wang C: High-mobility group protein B1 (HMGB1) is a novel biomarker for human ovarian cancer. Gynecol Oncol *126*: 109-117, 2012.

14 Ellerman JE, Brown CK, de Vera M, Zeh HJ, Billiar T, Rubartelli A and Lotze MT: Masquerader: high mobility group box-1 and cancer. Clin Cancer Res *13*: 2836-2848, 2007.

15 Kang R, Zhang Q, Zeh HJ, 3rd, Lotze MT and Tang D: HMGB1 in cancer: good, bad, or both? Clin Cancer Res *19*: 4046-4057, 2013.

16 Tang D, Kang R, Zeh HJ, 3rd and Lotze MT: High-mobility group box 1 and cancer. Biochim Biophys Acta *1799*: 131-140, 2010.

17 Washington MK: Colorectal carcinoma: selected issues in pathologic examination and staging and determination of prognostic factors. Arch Pathol Lab Med *132*: 1600-1607, 2008.
18 Volp K, Brezniceanu ML, Bosser S, Brabletz T, Kirchner T, Gottel D, Joos S and Zornig M: Increased expression of high mobility group box 1 (HMGB1) is associated with an elevated level of the antiapoptotic c-IAP2 protein in human colon carcinomas. Gut *55*: 234-242, 2006.
19 Xiang YY, Wang DY, Tanaka M, Suzuki M, Kiyokawa E, Igarashi H, Naito Y, Shen Q and Sugimura H: Expression of high-mobility group-1 mRNA in human gastrointestinal adenocarcinoma and corresponding non-cancerous mucosa. Int J Cancer *74*: 1-6, 1997.
20 Lange SS and Vasquez KM: HMGB1: the jack-of-all-trades protein is a master DNA repair mechanic. Mol Carcinog *48*: 571-580, 2009.
21 Travers AA: Priming the nucleosome: a role for HMGB proteins? EMBO Rep *4*: 131-136, 2003.
22 Lotze MT and Tracey KJ: High-mobility group box 1 protein (HMGB1): nuclear weapon in the immune arsenal. Nat Rev Immunol *5*: 331-342, 2005.
23 Taguchi A, Blood DC, del Toro G, Canet A, Lee DC, Qu W, Tanji N, Lu Y, Lalla E, Fu C, Hofmann MA, Kislinger T, Ingram M, Lu A, Tanaka H, Hori O, Ogawa S, Stern DM and Schmidt AM: Blockade of RAGE-amphoterin signalling suppresses tumour growth and metastases. Nature *405*: 354-360, 2000.
24 Tang D, Kang R, Coyne CB, Zeh HJ and Lotze MT: PAMPs and DAMPs: signal 0s that spur autophagy and immunity. Immunol Rev *249*: 158-175, 2012.

Received June 20, 2014
Revised July 22, 2014
Accepted July 23, 2014

Instructions to Authors 2014

General Policy. ANTICANCER RESEARCH (AR) will accept original high quality works and reviews on all aspects of experimental and clinical cancer research. The Editorial Policy suggests that priority will be given to papers advancing the understanding of cancer causation, and to papers applying the results of basic research to cancer diagnosis, prognosis, and therapy. AR will also accept the following for publication: (a) Abstracts and Proceedings of scientific meetings on cancer, following consideration and approval by the Editorial Board; (b) Announcements of meetings related to cancer research; (c) Short reviews (of approximately 120 words) and announcements of newly received books and journals related to cancer, and (d) Announcements of awards and prizes.

The principal aim of AR is to provide prompt publication (print and online) for original works of high quality, generally within 1-2 months from final acceptance. Manuscripts will be accepted on the understanding that they report original unpublished works on the cancer problem that are not under consideration for publication by another journal, and that they will not be published again in the same form. All authors should sign a submission letter confirming the approval of their article contents. All material submitted to AR will be subject to review, when appropriate, by two members of the Editorial Board and by one suitable outside referee. The Editors reserve the right to improve manuscripts on grammar and style.

The Editors and Publishers of AR accept no responsibility for the contents and opinions expressed by the contributors. Authors should warrantee due diligence in the creation and issuance of their work.

NIH Open Access Policy. The journal acknowledges that authors of NIH funded research retain the right to provide a copy of the final manuscript to the NIH four months after publication in ANTICANCER RESEARCH, for public archiving in PubMed Central.

Copyright. Once a manuscript has been published in ANTICANCER RESEARCH, which is a copyrighted publication, the legal ownership of all published parts of the paper has been transferred from the Author(s) to the journal. Material published in the journal may not be reproduced or published elsewhere without the written consent of the Managing Editor or Publisher.

Format. Two types of papers may be submitted: (i) Full papers containing completed original work, and (ii) review articles concerning fields of recognisable progress. Papers should contain all essential data in order to make the presentation clear. Reasonable economy should be exercised with respect to the number of tables and illustrations used. Papers should be written in clear, concise English. Spelling should follow that given in the "Shorter Oxford English Dictionary".

Manuscripts. Submitted manuscripts should not exceed fourteen (14) pages (approximately 250 words per double - spaced typed page), including abstract, text, tables, figures, and references (corresponding to 4 printed pages). Papers exceeding four printed pages will be subject to excess page charges. All manuscripts should be divided into the following sections:
(a) *First page* including the title of the presented work [not exceeding fifteen (15) words], full names and full postal addresses of all Authors, name of the Author to whom proofs are to be sent, key words, an abbreviated running title, an indication "review", "clinical", "epidemiological", or "experimental" study, and the date of submission. (Note: The order of the Authors is not necessarily indicative of their contribution to the work. Authors may note their individual contribution(s) in the appropriate section(s) of the presented work); (b) *Abstract* not exceeding 150 words, organized according to the following headings: Background/Aim - Materials and Methods/Patients and Methods - Results - Conclusion; (c) *Introduction;* (d) *Materials and Methods/Patients and Methods;* (e) *Results;* (f) *Discussion;* (g) *Acknowledgements;* (h) *References*. All pages must be numbered consecutively. Footnotes should be avoided. Review articles may follow a different style according to the subject matter and the Author's opinion. Review articles should not exceed 35 pages (approximately 250 words per double-spaced typed page) including all tables, figures, and references.

Figures. All figures (whether photographs or graphs) should be clear, high contrast, at the size they are to appear in the journal: 8.00 cm (3.15 in.) wide for a single column; 17.00 cm (6.70 in.) for a double column; maximum height: 20.00 cm (7.87 in.). Graphs must be submitted as photographs made from drawings and must not require any artwork, typesetting, or size modifications. Symbols, numbering and lettering should be clearly legible. The number and top of each figure must be indicated. Colour plates are charged.

Tables. Tables should be typed double-spaced on a separate page, numbered with Roman numerals and should include a short title.

References. Authors must assume responsibility for the accuracy of the references used. Citations for the reference sections of submitted works should follow the standard form of "Index Medicus" and must be numbered consecutively. In the text, references should be cited by number. Examples: 1 Sumner AT: The nature of chromosome bands and their significance for cancer research. Anticancer Res 1: 205-216, 1981. 2 McGuire WL and Chamnes GC: Studies on the oestrogen receptor in breast cancer. In: Receptors for Reproductive Hormones (O' Malley BW, Chamnes GC (eds.). New York, Plenum Publ Corp., pp 113-136, 1973.

Nomenclature and Abbreviations. Nomenclature should follow that given in "Chemical Abstracts", "Index Medicus", "Merck Index", "IUPAC –IUB", "Bergey's Manual of Determinative Bacteriology", The CBE Manual for Authors, Editors and Publishers (6th edition, 1994), and MIAME Standard for Microarray Data. Human gene symbols may be obtained from the HUGO Gene Nomenclature Committee (HGNC) (http://www.gene.ucl.ac.uk/). Approved mouse nomenclature may be obtained from http://www.informatics.jax.org/. Standard abbreviations are preferable. If a new abbreviation is used, it must be defined on first usage.

Clinical Trials. Authors of manuscripts describing clinical trials should provide the appropriate clinical trial number in the correct format in the text.

For International Standard Randomised Controlled Trials (ISRCTN) Registry (a not-for-profit organization whose registry is administered by Current Controlled Trials Ltd.) the unique number must be provided in this format: ISRCTNXXXXXXXX (where XXXXXXXX represents the unique number, always prefixed by "ISRCTN"). Please note that there is no space between the prefix "ISRCTN" and the number. Example: ISRCTN47956475.

For Clinicaltrials.gov registered trials, the unique number must be provided in this format: NCTXXXXXXXX (where XXXXXXXX represents the unique number, always prefixed by 'NCT'). Please note that there is no space between the prefix 'NCT' and the number. Example: NCT00001789.

Ethical Policies and Standards. ANTICANCER RESEARCH agrees with and follows the "Uniform Requirements for Manuscripts Submitted to Biomedical Journals" established by the International Committee of Medical Journal Editors in 1978 and updated in October 2001 (www.icmje.org). Microarray data analysis should comply with the "Minimum Information About Microarray Experiments (MIAME) standard". Specific guidelines are provided at the "Microarray Gene Expression Data Society" (MGED) website. Presentation of genome sequences should follow the guidelines of the NHGRI Policy on Release of Human Genomic Sequence Data. Research involving human beings must adhere to the principles of the Declaration of Helsinki and Title 45, U.S. Code of Federal Regulations, Part 46, Protection of Human Subjects, effective December 13, 2001. Research involving animals must adhere to the Guiding Principles in the Care and Use of Animals approved by the Council of the American Physiological Society. The use of animals in biomedical research should be under the careful supervision of a person adequately trained in this field and the animals must be treated humanely at all times. Research involving the use of human foetuses, foetal tissue, embryos and embryonic cells should adhere to the U.S. Public Law 103-41, effective December 13, 2001.

Submission of Manuscripts. Please follow the Instructions to Authors regarding the format of your manuscript and references. There are 3 ways to submit your article (NOTE: Please use only one of the 3 options. Do not send your article twice.):

1. To submit your article online please visit: IIAR-Submissions (http://www.iiar-anticancer.org/submissions/login.php)
2. You can send your article via e-mail to journals@iiar-anticancer.org. Please remember to always indicate the name of the journal you wish to submit your paper. The text should be sent as a Word document (*doc) attachment. Tables, figures and cover letter can also be sent as e-mail attachments.
3. You can send the manuscript of your article via regular mail in a USB stick, DVD, CD or floppy disk (including text, tables and figures) together with three hard copies to the following address:
   John G. Delinasios
   International Institute of Anticancer Research (IIAR)
   Editorial Office of ANTICANCER RESEARCH,
   IN VIVO, CANCER GENOMICS and PROTEOMICS.
   1st km Kapandritiou-Kalamou Road
   P.O. Box 22, GR-19014 Kapandriti, Attiki
   GREECE

Submitted articles will not be returned to Authors upon rejection.

Galley Proofs. Unless otherwise indicated, galley proofs will be sent to the first-named Author of the submission. Corrections of galley proofs should be limited to typographical errors. Reprints, PDF files, and/or Open Access may be ordered after the acceptance of the paper. Requests should be addressed to the Editorial Office.

FULL PAPER

BJC

British Journal of Cancer (2014) 110, 164–171 | doi: 10.1038/bjc.2013.698

Keywords: colorectal cancer; *PVT-1*; long noncoding RNA; apoptosis; 8q24

Amplification of *PVT-1* is involved in poor prognosis via apoptosis inhibition in colorectal cancers

Y Takahashi[1,2], G Sawada[1,2], J Kurashige[1], R Uchi[1], T Matsumura[1,2], H Ueo[1], Y Takano[1], H Eguchi[1], T Sudo[1], K Sugimachi[1], H Yamamoto[2], Y Doki[2], M Mori[2] and K Mimori*[,1]

[1]*Department of Surgery, Kyushu University Beppu Hospital, Tsurumihara 4546, Beppu 874-0838, Japan and* [2]*Department of Gastroenterological Surgery, Graduate School of Medicine, Osaka University, 2-2 Yamadaoka, Suita 565-0871, Japan*

Background: We previously conducted gene expression microarray analyses to identify novel indicators for colorectal cancer (CRC) metastasis and prognosis from which we identified *PVT-1* as a candidate gene. *PVT-1*, which encodes a long noncoding RNA, mapped to chromosome 8q24 whose copy-number amplification is one of the most frequent events in a wide variety of malignant diseases. However, *PVT-1* molecular mechanism of action remains unclear.

Methods: We conducted cell proliferation and invasion assays using colorectal cancer cell lines transfected with *PVT-1*siRNA or negative control siRNA. Gene expression microarray analyses on these cell lines were also carried out to investigate the molecular function of *PVT-1*. Further, we investigated the impact of *PVT-1* expression on the prognosis of 164 colorectal cancer patients by qRT–PCR.

Results: CRC cells transfected with *PVT-1* siRNA exhibited significant loss of their proliferation and invasion capabilities. In these cells, the TGF-β signalling pathway and apoptotic signals were significantly activated. In addition, univariate and multivariate analysis revealed that *PVT-1* expression level was an independent risk factor for overall survival of colorectal cancer patients.

Conclusion: *PVT-1*, which maps to 8q24, generates antiapoptotic activity in CRC, and abnormal expression of *PVT-1* was a prognostic indicator for CRC patients.

To identify novel indicators for colorectal cancer (CRC) metastasis and prognosis, we previously conducted gene expression array analysis using clinical samples resulting in the identification of several genes, which are involved in cancer progression and metastasis (Takahashi *et al*, 2013). The candidate genes include the *PVT-1* oncogene (*PVT-1*), which encodes a long noncoding RNA (lncRNA) and maps to chromosome 8q24 (8q24) (Carninci *et al*, 2005; Amaral *et al*, 2008; Guttman *et al*, 2009). Amplification of 8q24 is one of the most frequent events in a wide variety of malignant diseases including CRC, and has been associated with reduced survival duration in several studies (Popescu and Zimonjic, 2002; Lancaster *et al*, 2004; Guan *et al*, 2007). In addition to *PVT-1*, the well-established oncogene *MYC* has also been mapped to 8q24, and these two genes are co-amplified in CRC cell lines (Shtivelman and Bishop, 1989).

lncRNAs were previously believed to represent random transcriptional noise. However, their expression levels have been observed to vary spatially, temporally and in response to various stimuli (Mercer *et al*, 2009; Ponting *et al*, 2009). Moreover, several lncRNAs exhibit very precise expression patterns in different tissues (Amaral and Mattick, 2008; Mercer *et al*, 2008). In spite of emerging evidence, our understanding of the functions of these lncRNAs is limited. *PVT-1* produces a wide variety of spliced noncoding RNAs as well as a cluster of six annotated microRNAs: *miR-1204*, *miR-1205*, *miR-1206*, *miR-1207-5p*, *miR-1207-3p* and *miR-1208* (Barsotti *et al*, 2012). However, *PVT-1* exerts its

*Correspondence: Professor K Mimori; E-mail: kmimori@beppu.kyushu-u.ac.jp

Received 8 July 2013; revised 8 October 2013; accepted 11 October 2013; published online 5 November 2013

influence as an lncRNA (Guan *et al*, 2007; Alvarez and DiStefano, 2011; You *et al*, 2011). The molecular mechanism of *PVT-1* transcripts in gene regulation remains unclear. In the current study, we investigated the clinical significance of *PVT-1* expression in CRC.

MATERIALS AND METHODS

Patients and sample collection. We used a total of 312 CRC samples, of which 148 (set 1) were used as pure cancer tissues separated by laser microdissection (all cases were used for gene expression array and 130 cases were used for array-CGH), and 164 (set 2) were used in bulk for quantitative reverse transcription–PCR. All samples were obtained during surgery from patients who underwent resection of the primary tumour at Kyushu University Hospital at Beppu and affiliated hospitals between 1992 and 2007. Written informed consent was obtained from all patients. All patients had a clear histological diagnosis of CRC and were closely followed up every 3 months. The follow-up period in set 1 ranged from 0.1 months to 3.2 years with a mean of 2.1 years; follow-up in set 2 ranged from 0.1 to 12.3 years, with a mean of 3.8 years. Resected cancer tissues were immediately cut and stored in RNAlater (Ambion, Palo Alto, CA, USA) or embedded in Tissue-Tek OCT (optimum cutting temperature) medium (Sakura, Tokyo, Japan), frozen in liquid nitrogen and kept at −80 °C until DNA and RNA extraction. For DNA extraction, the QIAamp DNA Micro Kit (Qiagen, Hilden, Germany) was used following the manufacturer's protocol. For RNA extraction, frozen tissue specimens were homogenised in guanidinium thiocyanate, and total RNA was obtained by ultracentrifugation through a caesium chloride cushion. cDNA for reverse transcription–PCR was synthesised from 8.0 μg of total RNA with M-MLV Reverse Transcriptase (Invitrogen, Carlsbad, CA, USA). Clinicopathological factors and clinical stage were classified using the TNM system of classification. All sample data, including age, gender, histology, tumour depth, lymph node metastasis, lymphatic invasion, vascular invasion, liver metastasis and postoperative liver recurrence, were obtained from the clinical and pathological records.

Laser microdissection. Tissue samples were microdissected using an LMD6000 laser microdissection system (Leica Laser Microdissection System; Leica Microsystems, Wetzlar, Germany). For LMD, 5 μm-thick frozen sections were fixed in 70% ethanol for 30 s, stained with hematoxylin and eosin and de-hydrated as follows: 5 s each in 70%, 95% and 100% ethanol. Sections were air dried and then microdissected with the LMD system. Target cells were excised, with at least 100 cells per section, and bound to the transfer film. Total RNA was then extracted.

Quantitative real-time reverse transcription–PCR. For quantitative real-time reverse transcription (qRT)–PCR, *PVT-1* (NR_003367.1) primer sequences were 5′-TGAGAACTGTCCTTACGTGACC-3′ and 5′-AGAGCACCAAGACTGGCTCT-3′, and *MYC* (NM_002467.4) primer sequences were 5′-CACCAGCAGCGACTCTGA-3′ and 5′-GATCCAGACTCTGACCTTTTGC-3′. To normalise for RNA concentration, glyceraldehyde-3-phosphate dehydrogenase (*GAPDH*) served as an internal control. The sequences of the *GAPDH* primers were sense, 5′-TTGGTATCGTGGAAGGACTCA-3′ and antisense, 5′-TGTCATCATATTTGGCAGGTT-3′. The amplification protocol included an initial denaturation step at 95 °C for 10 min, followed by 45 cycles of 95 °C for 10 s and 60 °C for 30 s. qRT–PCR was performed in a LightCycler 480 instrument (Roche Applied Science, Basel, Switzerland) using the LightCycler 480 Probes Master kit (Roche Applied Science). All concentrations were calculated relative to the concentration of cDNA using Human Universal Reference Total RNA (Clontech, Palo Alto, CA, USA). The concentration of *PVT-1* was then divided by the concentration of the endogenous reference (*GAPDH*) to obtain normalised expression values. For qRT–PCR, for *miR-1204*, *miR-1205*, *miR-1206*, *miR-1207-3p*, *miR-1207-5p* and *miR-1208*, cDNA was synthesised from total RNA using TaqMan MicroRNA specific primers for each microRNAs (Applied Biosystems, Foster City, CA, USA) and a TaqMan MicroRNA Reverse Transcription kit (Applied Biosystems). Expression of target miRNAs was normalised to the expression of a small nuclear RNA, *RNU6B* (Applied Biosystems).

Cell lines. The human colorectal cancer cell lines RKO and HCT116 were obtained from the Japanese Cancer Research Bank (Tokyo, Japan) and maintained in Dulbecco's modified Eagle's medium containing 10% fetal bovine serum, 100 units ml^{-1} penicillin and 100 μg ml^{-1} streptomycin sulphate. All cells were cultured in a humidified 5% CO_2 incubator at 37 °C.

PVT-1 siRNA transfection. *PVT-1*-specific siRNAs (*PVT-1*siRNA-1: sense GCUUGGAGGCUGAGGAGUUTT and antisense AACUCCUCAGCCUCCAAGCTT and *PVT-1* siRNA-2: sense CCCAACAGGAGGACAGCUUTT and antisense AAGCUGUCCUCCUGUUGGGTT) and negative control siRNA were purchased from Cosmo Bio (Tokyo, Japan). siRNA oligonucleotide (30 nmol l^{-1}) in Opti-MEM (Invitrogen) were transfected into RKO and HCT116 cells using Lipofectamine RNAiMAX (Invitrogen) following the manufacturer's protocol. Cells in logarithmic growth phase were diluted without antibiotics and were seeded at 2×10^5 or 5×10^4 cells per well in a final volume of 2 ml or 500 μl, respectively, in 6- or 24-well flat-bottom microtiter plates, respectively. The cells were incubated in a humidified atmosphere (37 °C and 5% CO_2) for 24 h before use in assays.

Cell proliferation assay and cell invasion assay. To conduct the cell proliferation assay, 10 μl of MTT-labelling reagent (at a final concentration of 0.5 mg ml^{-1}) was added to each well, and the plate was incubated for 4 h in a humidified atmosphere. Solubilisation solution (100 μl) was added to each well, and the plate was incubated overnight in a humidified atmosphere. After confirming that the purple formazan crystals were completely solubilised, the absorbance of each well was measured using a Model 550 series microplate reader (Bio-Rad Laboratories, Hercules, CA, USA) at a wavelength of 570 nm corrected to 655 nm. The assay was performed using six replicates.

Invasion assays were done using the BD Biocoat Matrigel Invasion Chamber (pore size: 8 μm, 24-well; BD Biosciences, San Jose, CA, USA) following the manufacturer's protocol. A total of 5×10^4 cells were plated in the upper chamber in serum-free medium. The bottom chamber contained medium with 10% FBS. After 72 h, the bottom of the chamber insert was stained with Calcein AM (Invitrogen). The cells that had invaded through the membrane to the lower surface were evaluated in a fluorescence plate reader at excitation/emission wavelengths of 485/530 nm. Each assay was conducted in at least three replicates.

Western blotting. Total protein was extracted from each cell line. Aliquots of total protein (40 μg) were electrophoresed in 10% concentrated poly-acrylamide gel and then electrophoresed and then electroblotted as previously described (Ieta *et al*, 2007). The primary mouse monoclonal antibodies against caspase 3 (Cell Signaling Technology, Danvers, MA, USA), SMAD4 (Santa Cruz Biotechnbology, Dallas, TX, USA) were used at a dilution of 1 : 1000 and 1 : 200, respectively. Primary antibodies were detected using horseradish peroxidase (HRP)-conjugated secondary antibodies (GE Healthcare Japan, Tokyo, Japan) and the ImageQuant LAS 4000mini system (GE Healthcare Japan). Caspase 3 and SMAD4 proteins were normalised to the level of β-tubulin protein (Cell Signaling Technology) diluted 1 : 1000.

Array-CGH and copy-number analysis. A total of 130 tumour samples were prepared for array-CGH analysis. For genome profiling, the labelling and hybridisation of genomic DNA onto the Agilent Human Genome Microarray Kit 244 K (Agilent Technologies, Santa Clara, CA, USA) were performed according to the manufacturer's instructions. The raw signal intensities were measured and transformed into log ratios to reference DNA with 'Feature Extraction' software (version 9.1) from Agilent Technologies. Arrays were analysed using the Agilent DNA microarray scanner. The log ratio was thereafter used as the signal intensity of each probe. The raw copy-number data for each sample provided by array CGH was analysed using the GISTIC algorithm (Beroukhim *et al*, 2007; Mermel *et al*, 2011).

Gene expression array. The commercially available whole-Human Genome Microarray Kit and SurePrint G3 Human GE Microarray Kit (Agilent Technologies) were used to investigate globally altered genes. In brief, cyanine-labelled cRNA was prepared using the T7 linear amplification technique described in the Agilent Low RNA Input Fluorescent Linear Amplification Kit Manual (Agilent Technologies). Hundred nanograms of total RNA was extracted using the LMD technique and reverse transcribed to generate double-stranded cDNA using an oligo dT T7 promoter primer. Subsequently, cRNA was synthesised using T7 RNA polymerase, which simultaneously incorporated Cy3-labelled CTP. The quality of the cRNA was verified with the Agilent Bioanalyzer 2100. One microgram aliquots of Cy3-labelled cRNA were combined and fragmented in a hybridisation cocktail (Agilent Technologies). Labelled cRNA was then fragmented and hybridised to an oligonucleotide microarray. Fluorescence intensities were determined with an Agilent DNA microarray scanner. The gene expression profiles obtained from microarray data were quantile normalised. The batch effect in microarray experiments was also adjusted by an empirical Bayesian approach (Johnson *et al*, 2007).

Gene set enrichment analysis. For GSEA, *PVT-1* expression was treated as a numeric variable. We applied a continuous-type CLS file of the *PVT-1* profile to phenotype labels in GSEA. The metric for ranking genes in GSEA was set as 'pearson,' and the other parameters were set to their default values (Subramanian *et al*, 2005).

Statistical analysis. For continuous variables, data were expressed as means ± s.d. The relationship between *PVT-1* expression and clinicopathological factors was analysed using a χ^2-test and Student's *t*-test. Findings were considered significant when the *P*-value was <0.05. Correlation coefficients were analysed using the Pearson product-moment correlation coefficient. All tests were performed using the JMP software (SAS Institute Inc., Cary, NC, USA).

RESULTS

8q24 copy-number amplification and *PVT-1* expression. First, we applied array-CGH and gene expression array analyses on 130

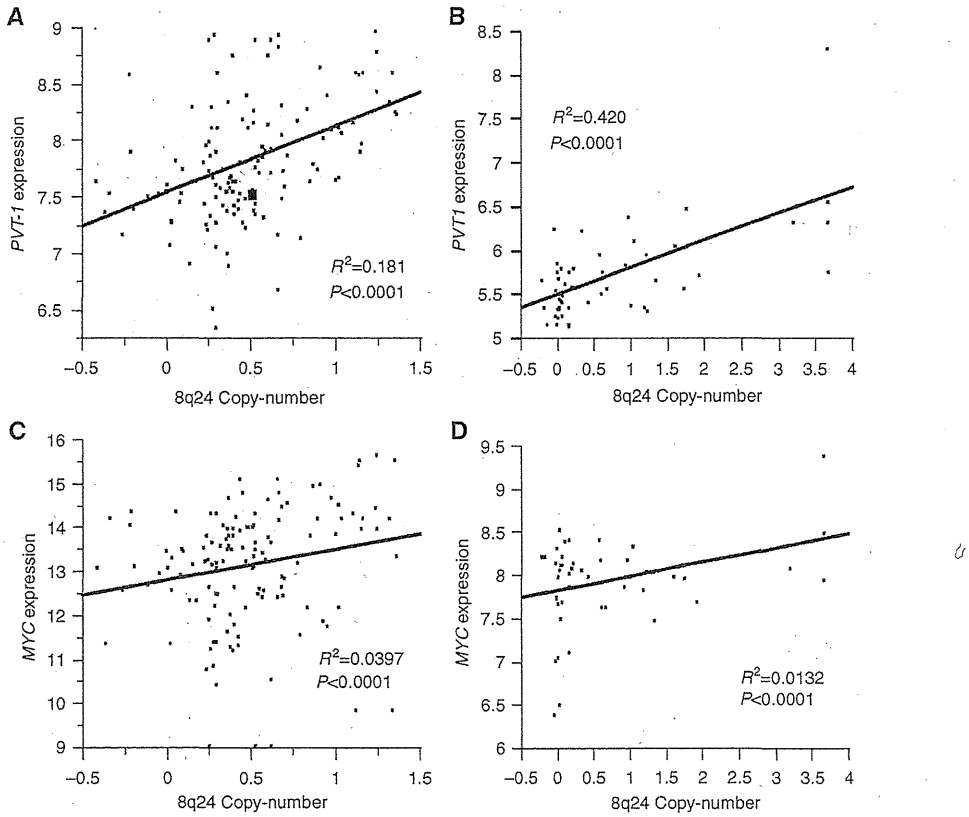

Figure 1. Positive correlation between chromosome 8q24 copy-number and *PVT-1* or *MYC* expression. (**A**) Chromosome 8q24 copy-number (horizontal axis) and *PVT-1* expression (vertical axis) analysed by array-CGH and gene expression array in 130 colorectal cancer cases. Dot plots indicate each case. (**B**) Chromosome 8q24 copy-number (horizontal axis) and *PVT-1* expression (vertical axis) in 50 colorectal cancer cell lines (the Cancer Cell Line Encyclopedia database). Dot plots indicate each cell line. (**C**) Chromosome 8q24 copy-number (horizontal axis) and *MYC* expression (vertical axis) analysed by array-CGH and gene expression array in 130 colorectal cancer cases. Dot plots indicate each case. (**D**) Chromosome 8q24 copy-number (horizontal axis) and *MYC* expression (vertical axis) in 50 colorectal cancer cell lines (the CCLE database). Dot plots indicate each cell line.

CRC tumours to investigate the correlation between chromosome 8q24 copy-number and *PVT-1* expression, and significant correlation was observed (Figure 1A; $R^2 = 0.181$, $P < 0.0001$). This result was validated with the Cancer Cell Line Encyclopedia (CCLE, http://www.broadinstitute.org/ccle/home), which is a recently compiled public resource that contains gene expression and chromosomal copy-number data from nearly 1000 cancer cell lines(Barretina *et al*, 2012). A significant positive correlation between 8q24 copy-number and *PVT-1* expression was also observed in 50 CRC cell lines (Figure 1B; $R^2 = 0.420$, $P < 0.0001$). These findings showed that 8q24 copy-number gain promoted *PVT-1* expression and suggested that aberrant expression of *PVT-1*, which we previously identified to be a candidate gene for CRC metastasis and progression (Takahashi *et al*, 2013), was of significance accompanied by genomic alteration in CRC. As *MYC* is a well-established oncogene, which also maps to 8q24, we investigated the correlation between 8q24 copy-numbers and *MYC* expression. Copy-numbers of 8q24 and *MYC* expression were also positively correlated in CRC tissues and CRC cell lines. However, the correlation between *MYC* and 8q24 copy-numbers was weaker than that between *PVT-1* and 8q24 copy-numbers (Figures 1C and D).

Knockdown of *PVT-1* promotes apoptosis in colorectal cancer cell lines. Next, we conducted *PVT-1* knockdown assays using siRNA to investigate the biological function of *PVT-1* transcripts in CRC cells. Using qRT–PCR, we confirmed that *PVT-1* expression in RKO and HCT116 cells transfected with *PVT-1*-specific siRNA was significantly lower than that in cells transfected with the negative control siRNA (Figure 2A). Cell proliferation assays were carried out in RKO and HCT116 colorectal cancer cells transfected with *PVT-1* siRNA or negative control siRNA. Both RKO and HCT116 cell lines have 8q24 copy-number amplification and *PVT-1* upregulation according to the CCLE database. *PVT-1*

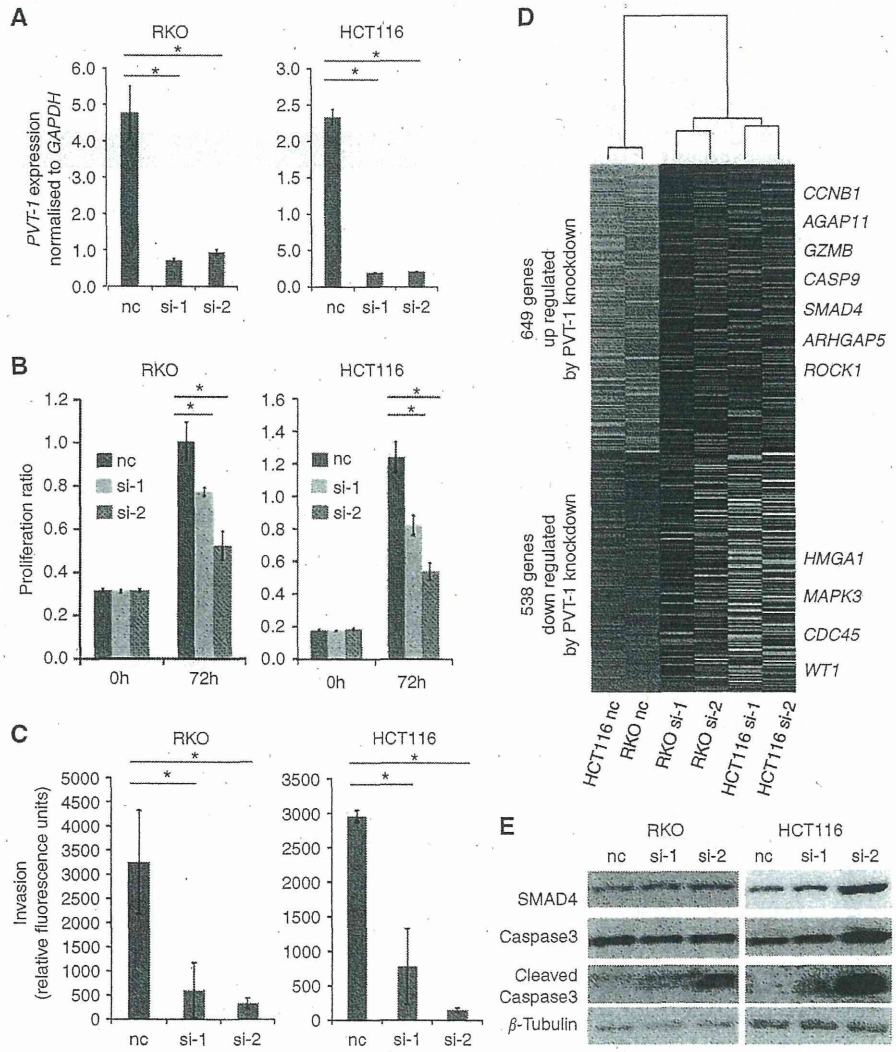

Figure 2. Knockdown of *PVT-1* promoted apoptosis in colorectal cancer cells. (**A**) qRT–PCR analysis showed that PVT-1 expression levels of both cell lines transfected with *PVT-1* siRNA were significantly lower than negative control (nc) cells. (**B**) Cell proliferation ratio of RKO cells (*left panel*) and HCT116 cells (*right panel*) with or without *PVT-1* knockdown. (**C**) Invasive properties of RKO cells (*left panel*) and HCT116 cells (*right panel*) with or without *PVT-1* knockdown. (**D**) A total of 1187 genes with significant alteration of expression levels (649 upregulated and 538 downregulated) by knockdown of *PVT-1*($P < 0.05$). Representative genes are shown in the right side of the heat map. (**E**) Western blot (left, RKO; right, HCT116) analyses of cells transfected with *PVT-1* siRNA, and negative control cells show the activation of SMAD4 and cleavage of caspase3. Histograms represent the means ± s.d. of three independent experiments. nc, cells transfected with negative control siRNA. si-1, cells transfected with *PVT-1* siRNA-1. si-2, cells transfected with *PVT-1* siRNA-2. *, statistically significant ($P < 0.05$).

knockdown significantly inhibited cancer cell proliferation in both cell lines (Figure 2B). This finding suggested that aberrant expression of *PVT-1* promoted the cell proliferation capability of colorectal cancer cells. Next, we conducted cancer cell invasion assays to verify the effect of *PVT-1* on metastasis, since we had originally identified *PVT-1* as a metastasis regulating gene. Then we observed that *PVT-1* siRNA transfected cells had reduced invasive abilities compared with negative control cells (Figure 2C).

To uncover the underlying mechanisms of anticancer activity of *PVT-1* knockdown, we performed gene expression microarray assays on cells transfected with *PVT-1* siRNA and negative control siRNA. A total of 649 genes including several apoptosis-relating genes were upregulated and 538 genes including some oncogenes were downregulated by *PVT-1* knockdown (Figure 2D, Supplementary Tables S1 and S2). Functional annotation analyses were performed using David Bioinformatics Resources 6.7, which is a web-based bioinformatics application (http://david.abcc.ncifcrf.gov/) (Imamichi *et al*, 2012), and we found that genes in the pathways for transforming growth factor beta (TGF-β) signalling and apoptosis were activated in cells with *PVT-1* knockdown (Supplementary Table S3). Actually, western blot analyses showed that the protein expression of SMAD4, which is in the TGF-β signalling pathway, was induced, and the cleavage of caspase 3 was observed in *PVT-1* knockdown cells (Figure 2E). These data showed that apoptosis was induced to CRC cells transfected with *PVT-1* siRNA via activation of TGF-β signalling. In order to confirm whether apoptosis was induced by knockdown of *PVT-1* lncRNA or by knockdown of microRNAs encoded by *PVT-1*, which seemed to be downregulated following knockdown of *PVT-1* transcripts, we conducted qRT–PCR assays for these six microRNAs in CRC cells transfected with *PVT-1* siRNA and negative control siRNA. Five of six microRNAs were detected by qRT–PCR, and no microRNAs were downregulated by *PVT-1* knockdown in CRC cells (Supplementary Figure S1).

PVT-1 expression is a prognostic indicator for colorectal cancer patients. *PVT-1* expression levels in 164 tumour tissues and corresponding normal tissues were examined by qRT–PCR to investigate the clinical significance of *PVT-1* in CRC. *PVT-1* expression levels in cancerous tissues were significantly higher than those in non-cancerous tissues ($P<0.0001$; Figure 3A). We divided the 164 patients with CRC into a high *PVT-1* expression group ($n=131$) and a low *PVT-1* expression group ($n=33$), classified as having expression levels higher or lower than the 20 percentile value, respectively, which is an approximation of the highest value among normal tissues. Clinicopathological factors were then analysed in the high and low *PVT-1* expression groups (Table 1). The high *PVT-1* expression group showed greater lymph node metastasis and venous invasion compared with the low *PVT-1* expression group. With regard to overall survival, patients with high *PVT-1* expression had a significantly poorer prognosis than those with low *PVT-1* expression ($P=0.0101$; Figure 3B). Univariate and multivariate analysis showed that *PVT-1* expression level was an independent prognostic indicator of overall survival in patients with CRC (relative risk: 2.532, $P=0.016$; Table 2). The clinical significance of *MYC* expression was also investigated in the same 164 colorectal cancer cases, as *MYC* is another important oncogene that maps to 8q24. *MYC* expression levels in cancerous tissues were significantly higher than those in non-cancerous tissues ($P<0.0001$; Figure 3C). In addition, we analysed the impact

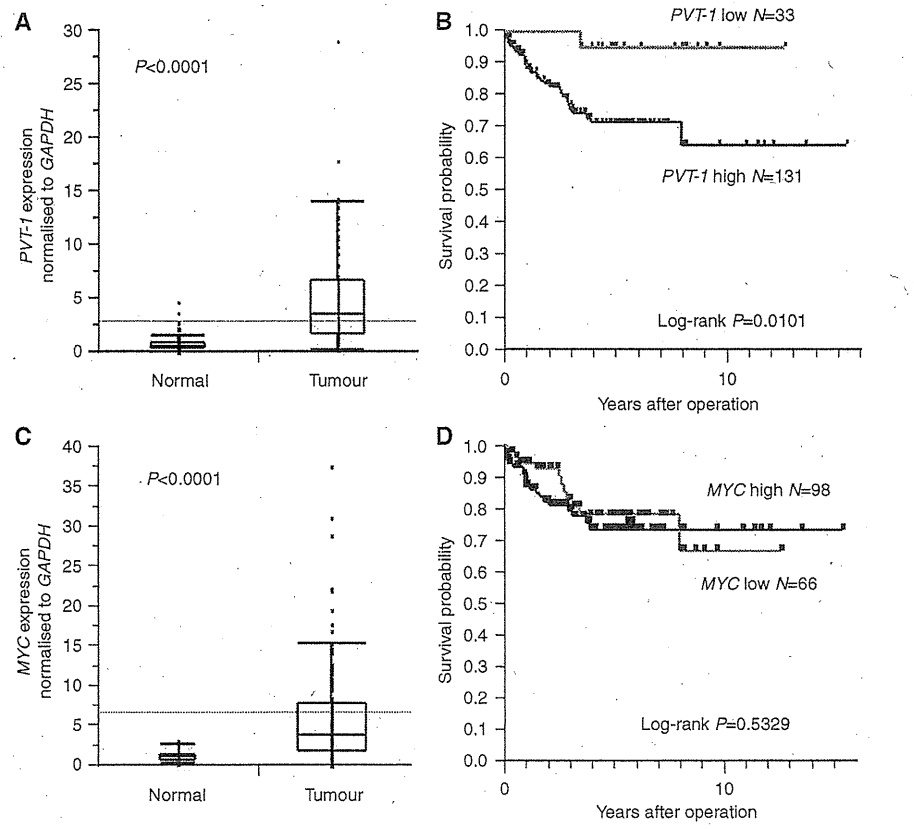

Figure 3. Abundant *PVT-1* expression is involved in poor prognosis in colorectal cancer. (**A**) qRT–PCR analyses of *PVT-1*expression levels on tumour tissues and paired normal tissues from 164 colorectal cancer samples. (**B**) Kaplan–Meier overall survival curves for 164 patients with CRC classified according to *PVT-1* expression level. (**C**) qRT–PCR analyses of *MYC* expression levels on tumour tissues and paired normal tissues from 164 colorectal cancer samples. (**D**) Kaplan–Meier overall survival curves for 164 patients with CRC classified according to *MYC* expression level.

Table 1. PVT-1 expression and clinicopathological factors in 164 colorectal cancer cases

		Low expression		High expression		
		$n=33$		$n=131$		
Factors		Number	%	Number	%	*P*-value
Age (y)	<65	10	30.30%	48	36.64%	0.4922
	>66	23	69.70%	83	63.36%	
Sex	Male	19	57.58%	78	59.54%	0.8375
	Female	14	42.42%	53	40.46%	
Histological grade	Well/moderate	31	93.94%	121	92.37%	0.7514
	other	2	6.06%	10	7.63%	
Tumour size	<30 mm	7	21.21%	33	25.19%	0.6303
	⩾30 mm	26	78.79%	98	74.81%	
Serosal invasion	Absent	12	36.36%	36	27.48%	0.3236
	Present	21	63.64%	95	72.52%	
Lymph node metastasis	N0	24	72.73%	62	47.33%	0.0079[a]
	N1-2	9	27.27%	69	52.67%	
Lymphatic invasion	Absent	24	72.73%	73	55.73%	0.0702
	Present	9	27.27%	58	44.27%	
Venous invasion	Absent	30	90.91%	100	76.34%	0.0472[a]
	Present	3	9.09%	31	23.66%	
Liver metastasis	Absent	32	96.97%	114	87.02%	0.0649
	Present	1	3.03%	17	12.98%	
Peritoneal dissemination	Absent	33	100.00%	123	93.89%	0.0545
	Present	0	0.00%	8	6.11%	
Distant metastasis	Absent	32	96.97%	128	97.71%	0.8104
	Present	1	3.03%	3	2.29%	
UICC Stage	0, I, II	24	72.73%	57	43.51%	0.0023[a]
	III, IV	9	27.27%	74	56.49%	

Abbreviations: Moderate = moderately differentiated tubular adenocarcinoma; UICC = Union for International Cancer Control; Well = well differentiated tubular adenocarcinoma.
[a]Statistically significant.

Table 2. Univariate and multivariate analysis for overall survival (Cox proportional hazards regression model)

	Univariate analysis			Multivariate analysis		
Factors	RR	95% CI	*P*-value	RR	95% CI	*P*-value
Age (< 65/66 <)	0.646	−0.800– −0.083	0.016[a]	—	—	—
Sex (male/female)	0.987	−0.380–0.341	0.944	—	—	—
Tumour size (< 30 mm/31 mm <)	2.078	0.187–1.173	0.012	1.616	0.931–2.540	0.083
Histology (well, moderate/others)	2.11	0.227–1.463	0.003[a]	1.365	0.799–2.820	0.28
Serosal invasion (absent/present)	4.218	0.669–2.879	<0.001[a]	2.788	1.237–11.920	0.009[a]
Lymphatic invasion (absent/present)	3.063	0.649–1.729	<0.001[a]	2.003	1.214–3.751	0.005[a]
Venous invasion (absent/present)	2.125	0.391–1.109	<0.001[a]	1.207	0.823–1.763	0.331
PVT-1 expression (low/high)	2.958	0.314–2.524	0.002[a]	2.532	1.152–10.747	0.016[a]

Abbreviations: CI = confidence interval; Moderate = moderately differentiated tubular; RR = relative risk; Well = well differentiated tubular adenocarcinoma.
[a]Statistically significant.

of *MYC* expression on colorectal cancer patients. We divided the 164 patients with colorectal cancer into a high *MYC* expression group ($n=98$) and a low *PVT-1* expression group ($n=66$), classified as having expression levels higher or lower than the 40 percentile value, respectively, which is an approximation of the highest *MYC* expression value among normal tissues. However, the

significance of *MYC* as a prognosticator for overall survival was not demonstrated in this case set (Figure 3D).

DISCUSSION

Several published reports have revealed that *PVT-1* is involved in cancer pathophysiology. In the current study, we focused on the clinical significance of aberrant *PVT-1* expression caused by copy-number amplification of chromosome 8q24. The *MYC* oncogene is also a notable oncogene mapping to 8q24 (Popescu and Zimonjic, 2002; Lancaster *et al*, 2004; Guan *et al*, 2007). However, the prognostic value of *MYC* expression was not verified in our case set. Although these data do not contradict the previously demonstrated significance of the *MYC* oncogene, the meaning of *PVT-1* in CRC pathophysiology was strongly suggested.

In our gene expression microarray analysis of CRC cell lines (Figure 2D), genes relating to the TGF-β signalling pathway were upregulated by *PVT-1* knockdown. *SMAD4*, a well-known tumour suppressor gene, is a major mediator of intracellular TGF-β signalling (Heldin *et al*, 1997; Massague, 1998) and inhibits tumour growth by inducing apoptosis in cancer cells (Brodin *et al*, 1999; Dai *et al*, 1999; Jang *et al*, 2002; Li *et al*, 2005). In the current study, *SMAD4* and apoptosis-relating genes were upregulated by *PVT-1* knockdown, suggesting that *PVT-1* knockdown promoted apoptosis via TGF-β signalling activation in CRC cells. On the other hand, *ROCK1*, which is another mediator of TGF-β signalling and promotes cancer invasiveness, was also activated in *PVT-1* knockdown cells. However, *PVT-1* knockdown cells lose their invasive capability (Figure 2B). We consider that this is because apoptosis has more impact on the phenotypes of CRC cells than *ROCK1* activation. Guan *et al*, have reported that *PVT-1* inhibits apoptosis independently of *MYC* in breast and ovarian cancer (Guan *et al*, 2007), and our results support their findings. However, the functions of microRNAs encoded by *PVT-1* must be taken into account. *miR-1207-5p* was an only microRNA deregulated by *PVT-1* knockdown, and the expression level of *miR-1207-5p* was upregulated following *PVT-1* knockdown (Supplementary Figure S1). *miR-1207-5p* was predicted to repress *CASP9*, using the microRNA target prediction online tool, TargetScan (http://www.targetscan.org/), which is involved in apoptosis signal and is one of the representative genes deregulated by *PVT-1* knockdown (shown in Figure 3D). Namely, *miR-1207-5p* was thought to inhibit apoptosis. Therefore, we consider that these microRNAs are regulated by other transcriptional mechanism and that these microRNAs are not involved in apoptosis induced by *PVT-1* knockdown.

Although only a small number of functional lncRNAs have been well characterised to date, emerging evidence has suggested that lncRNAs have roles as drivers of tumour suppressive or oncogenic functions in a wide variety of cancer types. In addition, many researchers have suggested mechanisms of action underlying the regulation of gene expression by lncRNAs (Wang and Chang, 2011). For example, lncRNAs can regulate chromosome structure *in cis* (Jonkers *et al*, 2008) or *in trans* (Rinn *et al*, 2007; Kogo *et al*, 2011). Other lncRNAs modulate the activity of protein-binding partners (Espinoza *et al*, 2004; Mariner *et al*, 2008). However, the molecular function of *PVT-1* is still controversial. However, we speculate that *PVT-1* regulates chromatin modification by targeting the SWItch/Sucrose NonFermentable (SWI/SNF) complex, which has tumour suppressive function (Roberts and Orkin, 2004; Tolstorukov *et al*, 2013). GSEA on clinical CRC samples suggested that *PVT-1* modulated the expression levels of target genes of SWI/SNF related, matrix associated, actin dependent regulator of chromatin, subfamily a, member 2 (*SMARCA2*) that constitute an ATPase subunit of SWI/SNF complex (Supplementary Figures S2A and B) and that *PVT-1* was associated with the apoptosis pathway (Supplementary Figures S2C). In addition, Shen *et al.* have reported the positive correlation between the expression of *SMARCA2*, *SMAD4* and other genes on the TGF-β pathway (Shen *et al*, 2008). Our *in vitro* study also supported these findings (Supplementary Figure S3). However, a limitation of this current study is that we did not demonstrate a direct molecular function of *PVT-1* in apoptosis induction clearly, and further investigation is needed.

In summary, we demonstrated that *PVT-1*, which encodes an lncRNA and maps to 8q24, generates antiapoptotic activity in colorectal cancer cells and that abnormal expression of *PVT-1* was a prognostic indicator for colorectal cancer patients. Further study is required to understand the underlying mechanism of apoptosis inhibition by *PVT-1*.

ACKNOWLEDGEMENTS

The present study was supported in part by the following grants and foundation; CREST, Japan Science and Technology Agency (JST), the Funding Program for Next Generation World-Leading Researchers (LS094), and Japan Society for the Promotion of Science (JSPS) Grant-in-Aid for Scientific Research, grant number 25861199. We thank T Shimooka, K Oda, M Kasagi, S Kono, T Kawano and M Aoyagi for their technical assistance.

CONFLICT OF INTEREST

The authors declare no conflict of interest.

REFERENCES

Alvarez ML, DiStefano JK (2011) Functional characterization of the plasmacytoma variant translocation 1 gene (PVT1) in diabetic nephropathy. *PLoS One* **6**(4): e18671.

Amaral PP, Dinger ME, Mercer TR, Mattick JS (2008) The eukaryotic genome as an RNA machine. *Science* **319**(5871): 1787–1789.

Amaral PP, Mattick JS (2008) Noncoding RNA in development. *Mamm Genome* **19**(7–8): 454–492.

Barretina J, Caponigro G, Stransky N, Venkatesan K, Margolin AA, Kim S, Wilson CJ, Lehar J, Kryukov GV, Sonkin D, Reddy A, Liu M, Murray L, Berger MF, Monahan JE, Morais P, Meltzer J, Korejwa A, Jane-Valbuena J, Mapa FA, Thibault J, Bric-Furlong E, Raman P, Shipway A, Engels IH, Cheng J, Yu GK, Yu J, Aspesi Jr P, de Silva M, Jagtap K, Jones MD, Wang L, Hatton C, Palescandolo E, Gupta S, Mahan S, Sougnez C, Onofrio RC, Liefeld T, Mac Conaill L, Winckler W, Reich M, Li N, Mesirov JP, Gabriel SB, Getz G, Ardlie K, Chan V, Myer VE, Weber BL, Porter J, Warmuth M, Finan P, Harris JL, Meyerson M, Golub TR, Morrissey MP, Sellers WR, Schlegel R, Garraway LA (2012) The Cancer Cell Line Encyclopedia enables predictive modelling of anticancer drug sensitivity. *Nature* **483**(7391): 603–607.

Barsotti AM, Beckerman R, Laptenko O, Huppi K, Caplen NJ, Prives C (2012) p53-Dependent induction of PVT1 and miR-1204. *J Biol Chem* **287**(4): 2509–2519.

Beroukhim R, Getz G, Nghiemphu L, Barretina J, Hsueh T, Linhart D, Vivanco I, Lee JC, Huang JH, Alexander S, Du J, Kau T, Thomas RK, Shah K, Soto H, Perner S, Prensner J, Debiasi RM, Demichelis F, Hatton C, Rubin MA, Garraway LA, Nelson SF, Liau L, Mischel PS, Cloughesy TF, Meyerson M, Golub TA, Lander ES, Mellinghoff IK, Sellers WR (2007) Assessing the significance of chromosomal aberrations in cancer: methodology and application to glioma. *Proc Natl Acad Sci USA* **104**(50): 20007–20012.

Brodin G, ten Dijke P, Funa K, Heldin CH, Landstrom M (1999) Increased smad expression and activation are associated with apoptosis in normal and malignant prostate after castration. *Cancer Res* **59**(11): 2731–2738.

Carninci P, Kasukawa T, Katayama S, Gough J, Frith MC, Maeda N, Oyama R, Ravasi T, Lenhard B, Wells C, Kodzius R, Shimokawa K,

Bajic VB, Brenner SE, Batalov S, Forrest AR, Zavolan M, Davis MJ, Wilming LG, Aidinis V, Allen JE, Ambesi-Impiombato A, Apweiler R, Aturaliya RN, Bailey TL, Bansal M, Baxter L, Beisel KW, Bersano T, Bono H, Chalk AM, Chiu KP, Choudhary V, Christoffels A, Clutterbuck DR, Crowe ML, Dalla E, Dalrymple BP, de Bono B, Della Gatta G, di Bernardo D, Down T, Engstrom P, Fagiolini M, Faulkner G, Fletcher CF, Fukushima T, Furuno M, Futaki S, Gariboldi M, Georgii-Hemming P, Gingeras TR, Gojobori T, Green RE, Gustincich S, Harbers M, Hayashi Y, Hensch TK, Hirokawa N, Hill D, Huminiecki L, Iacono M, Ikeo K, Iwama A, Ishikawa T, Jakt M, Kanapin A, Katoh M, Kawasawa Y, Kelso J, Kitamura H, Kitano H, Kollias G, Krishnan SP, Kruger A, Kummerfeld SK, Kurochkin IV, Lareau LF, Lazarevic D, Lipovich L, Liu J, Liuni S, McWilliam S, Madan Babu M, Madera M, Marchionni L, Matsuda H, Matsuzawa S, Miki H, Mignone F, Miyake S, Morris K, Mottagui-Tabar S, Mulder N, Nakano N, Nakauchi H, Ng P, Nilsson R, Nishiguchi S, Nishikawa S, Nori F, Ohara O, Okazaki Y, Orlando V, Pang KC, Pavan WJ, Pavesi G, Pesole G, Petrovsky N, Piazza S, Reed J, Reid JF, Ring BZ, Ringwald M, Rost B, Ruan Y, Salzberg SL, Sandelin A, Schneider C, Schonbach C, Sekiguchi K, Semple CA, Seno S, Sessa L, Sheng Y, Shibata Y, Shimada H, Shimada K, Silva D, Sinclair B, Sperling S, Stupka E, Sugiura K, Sultana R, Takenaka Y, Taki K, Tammoja K, Tan SL, Tang S, Taylor MS, Tegner J, Teichmann SA, Ueda HR, van Nimwegen E, Verardo R, Wei CL, Yagi K, Yamanishi H, Zabarovsky E, Zhu S, Zimmer A, Hide W, Bult C, Grimmond SM, Teasdale RD, Liu ET, Brusic V, Quackenbush J, Wahlestedt C, Mattick JS, Hume DA, Kai C, Sasaki D, Tomaru Y, Fukuda S, Kanamori-Katayama M, Suzuki M, Aoki J, Arakawa T, Iida J, Imamura K, Itoh M, Kato T, Kawaji H, Kawagashira N, Kawashima T, Kojima M, Kondo S, Konno H, Nakano K, Ninomiya N, Nishio T, Okada M, Plessy C, Shibata K, Shiraki T, Suzuki S, Tagami M, Waki K, Watahiki A, Okamura-Oho Y, Suzuki H, Kawai J, Hayashizaki Y, Consortium F. Group RGER, Genome Science G (2005) The transcriptional landscape of the mammalian genome. *Science* **309**(5740): 1559–1563.

Dai JL, Bansal RK, Kern SE (1999) G1 cell cycle arrest and apoptosis induction by nuclear Smad4/Dpc4: phenotypes reversed by a tumorigenic mutation. *Proc Natl Acad Sci USA* **96**(4): 1427–1432.

Espinoza CA, Allen TA, Hieb AR, Kugel JF, Goodrich JA (2004) B2 RNA binds directly to RNA polymerase II to repress transcript synthesis. *Nat Struct Mol Biol* **11**(9): 822–829.

Guan Y, Kuo WL, Stilwell JL, Takano H, Lapuk AV, Fridlyand J, Mao JH, Yu M, Miller MA, Santos JL, Kalloger SE, Carlson JW, Ginzinger DG, Celniker SE, Mills GB, Huntsman DG, Gray JW (2007) Amplification of PVT1 contributes to the pathophysiology of ovarian and breast cancer. *Clin Cancer Res* **13**(19): 5745–5755.

Guttman M, Amit I, Garber M, French C, Lin MF, Feldser D, Huarte M, Zuk O, Carey BW, Cassady JP, Cabili MN, Jaenisch R, Mikkelsen TS, Jacks T, Hacohen N, Bernstein BE, Kellis M, Regev A, Rinn JL, Lander ES (2009) Chromatin signature reveals over a thousand highly conserved large non-coding RNAs in mammals. *Nature* **458**(7235): 223–227.

Heldin CH, Miyazono K, ten Dijke P (1997) TGF-beta signalling from cell membrane to nucleus through SMAD proteins. *Nature* **390**(6659): 465–471.

Ieta K, Ojima E, Tanaka F, Nakamura Y, Haraguchi N, Mimori K, Inoue H, Kuwano H, Mori M (2007) Identification of overexpressed genes in hepatocellular carcinoma, with special reference to ubiquitin-conjugating enzyme E2C gene expression. *Int J Cancer* **121**(1): 33–38.

Imamichi T, Yang J, Huang da W, Sherman B, Lempicki RA (2012) Interleukin-27 induces interferon-inducible genes: analysis of gene expression profiles using Affymetrix microarray and DAVID. *Methods Mol Biol* **820**: 25–53.

Jang CW, Chen CH, Chen CC, Chen JY, Su YH, Chen RH (2002) TGF-beta induces apoptosis through Smad-mediated expression of DAP-kinase. *Nat Cell Biol* **4**(1): 51–58.

Johnson WE, Li C, Rabinovic A (2007) Adjusting batch effects in microarray expression data using empirical Bayes methods. *Biostatistics* **8**(1): 118–127.

Jonkers I, Monkhorst K, Rentmeester E, Grootegoed JA, Grosveld F, Gribnau J (2008) Xist RNA is confined to the nuclear territory of the silenced X chromosome throughout the cell cycle. *Mol Cell Biol* **28**(18): 5583–5594.

Kogo R, Shimamura T, Mimori K, Kawahara K, Imoto S, Sudo T, Tanaka F, Shibata K, Suzuki A, Komune S, Miyano S, Mori M (2011) Long noncoding RNA HOTAIR regulates polycomb-dependent chromatin modification and is associated with poor prognosis in colorectal cancers. *Cancer Res* **71**(20): 6320–6326.

Lancaster JM, Dressman HK, Whitaker RS, Havrilesky L, Gray J, Marks JR, Nevins JR, Berchuck A (2004) Gene expression patterns that characterize advanced stage serous ovarian cancers. *J Soc Gynecol Invest* **11**(1): 51–59.

Li Q, Wu L, Oelschlager DK, Wan M, Stockard CR, Grizzle WE, Wang N, Chen H, Sun Y, Cao X (2005) Smad4 inhibits tumor growth by inducing apoptosis in estrogen receptor-alpha-positive breast cancer cells. *J Biol Chem* **280**(29): 27022–27028.

Mariner PD, Walters RD, Espinoza CA, Drullinger LF, Wagner SD, Kugel JF, Goodrich JA (2008) Human Alu RNA is a modular transacting repressor of mRNA transcription during heat shock. *Mol Cell* **29**(4): 499–509.

Massague J (1998) TGF-beta signal transduction. *Annu Rev Biochem* **67**: 753–791.

Mercer TR, Dinger ME, Mattick JS (2009) Long non-coding RNAs: insights into functions. *Nat Rev Genet* **10**(3): 155–159.

Mercer TR, Dinger ME, Sunkin SM, Mehler MF, Mattick JS (2008) Specific expression of long noncoding RNAs in the mouse brain. *Proc Natl Acad Sci USA* **105**(2): 716–721.

Mermel CH, Schumacher SE, Hill B, Meyerson ML, Beroukhim R, Getz G (2011) GISTIC2.0 facilitates sensitive and confident localization of the targets of focal somatic copy-number alteration in human cancers. *Genome Biol* **12**(4): R41.

Ponting CP, Oliver PL, Reik W (2009) Evolution and functions of long noncoding RNAs. *Cell* **136**(4): 629–641.

Popescu NC, Zimonjic DB (2002) Chromosome-mediated alterations of the MYC gene in human cancer. *J Cell Mol Med* **6**(2): 151–159.

Rinn JL, Kertesz M, Wang JK, Squazzo SL, Xu X, Brugmann SA, Goodnough LH, Helms JA, Farnham PJ, Segal E, Chang HY (2007) Functional demarcation of active and silent chromatin domains in human HOX loci by noncoding RNAs. *Cell* **129**(7): 1311–1323.

Roberts CW, Orkin SH (2004) The SWI/SNF complex–chromatin and cancer. *Nat Rev Cancer* **4**(2): 133–142.

Shen H, Powers N, Saini N, Comstock CE, Sharma A, Weaver K, Revelo MP, Gerald W, Williams E, Jessen WJ, Aronow BJ, Rosson G, Weissman B, Muchardt C, Yaniv M, Knudsen KE (2008) The SWI/SNF ATPase Brm is a gatekeeper of proliferative control in prostate cancer. *Cancer Res* **68**(24): 10154–10162.

Shtivelman E, Bishop JM (1989) The PVT gene frequently amplifies with MYC in tumor cells. *Mol Cell Bio* **9**(3): 1148–1154.

Subramanian A, Tamayo P, Mootha VK, Mukherjee S, Ebert BL, Gillette MA, Paulovich A, Pomeroy SL, Golub TR, Lander ES, Mesirov JP (2005) Gene set enrichment analysis: a knowledge-based approach for interpreting genome-wide expression profiles. *Proc Natl Acad Sci USA* **102**(43): 15545–15550.

Takahashi Y, Sawada G, Sato T, Kurashige J, Mima K, Matsumura T, Uchi R, Ueo H, Ishibashi M, Takano Y, Akiyoshi S, Eguchi H, Sudo T, Sugimachi K, Tanaka J, Kudo S, Doki Y, Mori M, Mimori K (2013) Microarray analysis reveals that high mobility group A1 is involved in colorectal cancer metastasis. *Oncol Rep* **30**(3): 1488–1496.

Tolstorukov MY, Sansam CG, Lu P, Koellhoffer EC, Helming KC, Alver BH, Tillman EJ, Evans JA, Wilson BG, Park PJ, Roberts CW (2013) Swi/Snf chromatin remodeling/tumor suppressor complex establishes nucleosome occupancy at target promoters. *Proc Natl Acad Sci USA* **110**(25): 10165–10170.

Wang KC, Chang HY (2011) Molecular mechanisms of long noncoding RNAs. *Mol Cell* **43**(6): 904–914.

You L, Chang D, Du HZ, Zhao YP (2011) Genome-wide screen identifies PVT1 as a regulator of Gemcitabine sensitivity in human pancreatic cancer cells. *Biochem Biophys Res Commun* **407**(1): 1–6.

Supplementary Information accompanies this paper on British Journal of Cancer website (http://www.nature.com/bjc)

Ann Surg Oncol (2014) 21:205–212
DOI 10.1245/s10434-013-3264-3

Annals of
SURGICAL ONCOLOGY
OFFICIAL JOURNAL OF THE SOCIETY OF SURGICAL ONCOLOGY

ORIGINAL ARTICLE – COLORECTAL CANCER

Up-regulation of *NEK2* by *MicroRNA-128* Methylation is Associated with Poor Prognosis in Colorectal Cancer

Yusuke Takahashi, MD[1,2], Takeshi Iwaya, MD, PhD[1], Genta Sawada, MD[1,2], Junji Kurashige, MD, PhD[1], Tae Matsumura, MD[1,2], Ryutaro Uchi, MD[1], Hiroki Ueo, MD[1], Yuki Takano, MD[1], Hidetoshi Eguchi, MD, PhD[1], Tomoya Sudo, MD, PhD[1], Keishi Sugimachi, MD, PhD[1], Hirofumi Yamamoto, MD, PhD[2], Yuichiro Doki, MD, PhD[2], Masaki Mori, MD, PhD, FACS[2], and Koshi Mimori, MD, PhD[1]

[1]Department of Surgery, Beppu Hospital, Kyushu University, Beppu, Japan; [2]Department of Gastroenterological Surgery, Graduate School of Medicine, Osaka University, Suita, Japan

ABSTRACT

Background. NIMA-related kinase 2 (NEK2), an enzyme involved in the development and progression of cancer, is abnormally expressed in a wide variety of human cancers, including colorectal cancer (CRC), and is known to have roles in cell division and mitotic regulation through centrosome splitting. We investigated the clinical significance of *NEK2* in CRC. In particular, we examined *miR-128* expression, which is thought to target *NEK2*.

Methods. We measured *NEK2* mRNA and *miR-128* levels in clinical samples by quantitative reverse transcription real-time PCR and analyzed the associations between *NEK2* levels, *miR-128* levels, clinicopathological factors, and prognoses. Furthermore, we performed in vitro assays using a pre-*miR-128* precursor and conducted *miR-128* methylation analyses.

Results. *MiR-128* inhibited *NEK2* expression and cancer cell proliferation via cell cycle arrest. Moreover, *miR-128* was silenced by DNA methylation. Increased *NEK2* expression was associated with serosal invasion, lymphatic invasion, and peritoneal dissemination. Patients with high *NEK2* expression also had significantly poorer prognoses. Multivariate analysis indicated that high *NEK2* expression was an independent prognostic factor for survival. Patients with high *miR-128* expression had significantly lower *NEK2* expression and lower recurrence rates than those with low *miR-128* expression.

Conclusions. *NEK2* may be an independent prognostic factor for CRC and was regulated by *miR-128*, a microRNA that was subjected to epigenetic regulation. Thus, this *miR-128/NEK2* pathway may be a prospective therapeutic target for patients with CRC.

First Received: 10 June 2013;
Published Online: 18 September 2013

K. Mimori, MD, PhD
e-mail: kmimori@beppu.kyushu-u.ac.jp

NIMA-related kinase 2 (NEK2), a member of the Nek family of serine/threonine kinases, is structurally related to the essential mitotic regulator NIMA and is highly enriched at the centrosome.[1] NEK2 is involved in both the maintenance and modulation of the centrosome architecture. Moreover, NEK2 kinase activity promotes centrosomal splitting at the onset of mitosis and the G_2/M transition through phosphorylation of core centriolar proteins.[2–4] *NEK2* overexpression has been reported in a wide variety of human cancers, such as non-Hodgkin lymphoma,[5] breast cancer,[6–9] cervical cancer,[6] and prostate cancer.[6] In addition, *NEK2* has been shown to be involved in tumor progression, and *NEK2* depletion suppresses tumor cell growth, both in vitro and in vivo, in breast cancer,[8] cholangiocarcinoma,[10] and colorectal cancer (CRC) cell lines.[11]

According to the online predictive algorithm TargetScan 5.2 (http://www.targetscan.org/vert_50/), *microRNA-128* (*miR-128*) is the only microRNA that hypothetically targets *NEK2* and is thought to be a tumor suppressor. Reports have demonstrated that *miR-128* inhibits tumor cell proliferation in glioma, neuroblastoma, and prostate cancer.[12–15] In spite of their importance, however, the roles and interactions of *NEK2* and *miR-128* remain largely unclear. In the current study, we investigated the clinical importance of the *NEK2/miR-128* pathway in CRC.

MATERIALS AND METHODS

Patients and Sample Collection

One hundred eighty patients with CRC who underwent surgical treatment at Kyushu University at Beppu and affiliated hospitals between 1992 and 2002 were enrolled in this study. Resected tumor samples were immediately collected from resected colons, placed in RNAlater (Takara, Japan), frozen in liquid nitrogen, and stored at −80 °C until RNA extraction. The median follow-up period was 2.93 years. All data pertaining to the samples, including patient age and gender, tumor size and depth, lymphatic invasion, lymph node metastasis, vascular invasion, liver metastasis, peritoneal dissemination, distant metastasis, clinical stage, and histological grade, were obtained from clinical and pathological records. Written informed consent was obtained from all patients in accordance with the guidelines approved by the Institutional Research Board. This study was conducted under the supervision of the ethical board of Kyushu University and affiliated hospitals.

Cell Lines

The human CRC cell lines DLD-1, HCT116, HT29, and RKO were purchased from American Type Culture Collection and maintained in RPMI 1640 (for DLD-1, HCT116, and HT29) or Dulbecco's modified Eagle's Medium (for RKO) containing 10 % fetal bovine serum, 100 units/mL penicillin, and 100 μg/mL streptomycin sulfate. All cells were cultured in a humidified 5 % CO_2 incubator at 37 °C.

Transfection with NEK2 siRNA and miR-128 Precursor (Pre-miR-128)

DLD-1 or RKO cells (2×10^5) were transfected with 60 pmol *NEK2*-specific siRNA (siRNA No. 1102691) or negative control siRNA (Cosmo Bio, Tokyo, Japan), and 60 pmol pre-*miR-128* or pre-*miR* negative control (pre-*miR*, Ambion, Austin, TX, USA) using Lipofectamine RNAiMAX (Invitrogen Life Technologies, Carlsbad, CA, USA) according to the manufacturer's instructions.

RNA Preparation for Reverse-transcription PCR

Total RNA was isolated using a modified acid-guanidinium-phenol-chloroform procedure. Complementary DNA (cDNA) was synthesized from 8 μg total RNA using random hexamer primers and Moloney murine leukemia virus (M-MLV) reverse transcriptase (Invitrogen Life Technologies).

Evaluation of Gene and MicroRNA Expression in Clinical Samples

For quantitative real-time reverse transcription (qRT)-PCR, *NEK2* (NM_002497.2) primer sequences were as follows: sense, 5′-CATTGGCACAGGCTCCTAC-3′ and antisense, 5′-GAGCCATAGTCAAGTTCTTTCCA-3′. To normalize RNA concentrations between samples, glyceraldehyde-3-phosphate dehydrogenase (*GAPDH*) served as an internal control. The sequences of the *GAPDH* primers were as follows: sense, 5′-TTGGTATCGTGGAAGGA CTCA-3′ and antisense, 5′-TGTCATCATATTTGGCAGG TT-3′. The amplification protocol included an initial denaturation step at 95 °C for 10 min, followed by 45 cycles of 95 °C for 10 s and 60 °C for 30 s. qRT-PCR was performed in a LightCycler 480 instrument (Roche Applied Science, Basel, Switzerland) using the LightCycler 480 Probes Master kit (Roche Applied Science). All concentrations were calculated relative to the concentration of cDNA using Human Universal Reference Total RNA (Clontech, Palo Alto, CA, USA). The amount of *NEK2* was then divided by the amount of the endogenous reference (GAPDH) to obtain normalized expression values. For *miR-128* qRT-PCR, cDNA was synthesized from total RNA using TaqMan MicroRNA *miR-128* specific primers (Applied Biosystems, Foster City, CA, USA) and a TaqMan MicroRNA Reverse Transcription kit (Applied Biosystems). Expression of target miRNAs was normalized to the expression of a small nuclear RNA, *RNU6B* (Applied Biosystems).

Construction of Reporter Plasmids and Evaluation of Luciferase Reporter Activity

To construct a luciferase reporter plasmid, a *NEK2* 3′-untranslated region (UTR) full-length fragment was subcloned into the pmirGlo Dual-luciferase miRNA Target Expression Vector (Promega, Madison, WI, USA) located 5′ to the firefly luciferase. Nucleotide sequences of the constructed plasmids were confirmed by DNA sequencing analysis. For luciferase reporter assays, DLD-1 and RKO cells were seeded in 96-well plates and then cotransfected with the pmirGlo-*NEK2* 3′-UTR construct and *miR-128* (pre-*miR-128*) or pre-*miR* negative control (Ambion). Assays were conducted 48 h after transfection using the Dual-Luciferase Reporter Assay System (Promega). Firefly luciferase signals were normalized to Renilla luciferase signals. Transfections were conducted 3 times in independent experiments.

Immunoblotting Analysis

Total cellular protein was extracted from DLD-1 and RKO cells 48 h after transfection with pre-*miR-128*. Total protein

(40 μg) was subjected to electrophoresis and then electroblotted as previously described.[16] Protein was detected using primary anti-NEK2 antibodies (Abcam, Cambridge, UK) diluted 1:600, and primary antibodies were then detected using horseradish peroxidase (HRP)-conjugated secondary antibodies (GE Healthcare, Buckinghamshire, UK). NEK2 protein expression was normalized to the level of β-actin protein using specific antibodies (Cytoskeleton Inc., Denver, CO) diluted 1:1,000.

Cell Proliferation and Cell Cycle Analysis

Cell proliferation was evaluated by MTT assay using the Cell Proliferation Kit 1 (Roche Applied Science) according to the manufacturer's instructions. For cell cycle analysis, cells were fixed in 70 % ethanol at −20 °C, resuspended in PBS, and incubated for 15 min at 37 °C in PBS containing 10 μg/mL RNase A. Next, 10 μg/mL propidium iodide (PI) was added, and cells were incubated for 30 min at 24 °C. Data were collected on a FACSvantage cell sorter (Becton Dickinson, Franklin Lakes, NJ, USA).

DNA Methylation Analysis

To analyze the restored expression of genes and microRNAs of interest, cells were cultured with or without 2 mM 5-aza 2′-deoxycytidine (5-aza-dCyd) for 2 days. Genomic DNA was treated with sodium bisulfite using the MethylEasy Xceed Rapid DNA Bisulphite Modification Kit (Takara, Japan) according to the manufacturer's instructions and subjected to PCR using primer sets designed to amplify regions of interest. The sequences of

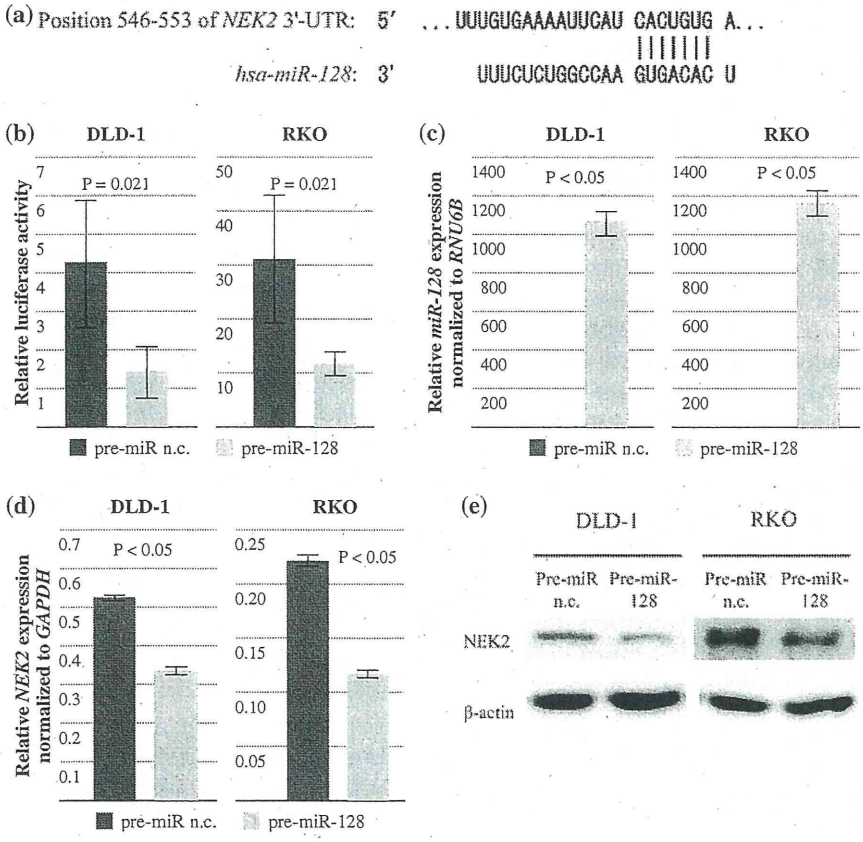

FIG. 1 *MiR-128* targeted *NEK2*. **a** Sequences of *miR-128* binding sites in the 3′-UTRs of transcripts encoding *NEK2*. **b** Luciferase assays demonstrated that *miR-128* repressed its target in DLD-1 cells (*left*) and RKO cells (*right*). Relative luciferase level = [(sample Luc/sample Renilla)/(control Luc/control Renilla)]. *Luc* raw firefly luciferase activity; *Renilla* internal transfection control Renilla activity. The error bar represents the SD from six replicates. **c** *miR-128/RNU6B* expression as measured by quantitative real-time PCR analysis in DLD-1 cells (*left*) and RKO cells (*right*) after transfection with pre-*miR-128*. Error bars represent the SD from three replicates. **d** *NEK2/GAPDH* expression as measured by quantitative real-time PCR analysis in DLD-1 cells (*left*) and RKO cells (*right*) after transfection with pre-*miR-128*. *Error bars* represent the SD from three replicates. **e** Western blot analysis for *NEK2* protein expression in cells transfected with the negative control or pre-*miR-128*. Protein expression was normalized to the expression of β-actin. *Pre-miR n.c.* pre-*miR* negative control

primers were as follows: sense, 5′-GAGAGGATTGTGGG TATAGAAG-3′, and antisense, 5′-AAATCCCACA-CAACTATAACAAC-3′. For bisulfite sequencing analysis, the PCR products were subcloned and then sequenced. DNA methylation status was analyzed using the quantification tool for methylation analysis (QUMA).[17]

Statistical Analysis

Data from RT-PCR analyses and in vitro transfected cell assays were analyzed using JMP 5 software (JMP, Cary, NC, USA). Overall survival rates were calculated actuarially according to the Kaplan–Meier method and were measured from the day of surgery. Differences between groups were estimated using the χ^2 test, Student's t test, repeated-measures ANOVA, and log-rank test. Variables with a P-value of less than 0.05 in univariate analysis were used in a subsequent multivariate analysis On the basis of the Cox proportional hazards model. A probability level of 0.05 was chosen for statistical significance.

RESULTS

MiR-128 Regulated NEK2 Expression in CRC Cells

Using the online tool, TargetScan, we identified the sequences of *miR-128* binding sites in the 3′-UTRs of transcripts encoding NEK2 (Fig. 1a). To investigate binding and repression, a luciferase reporter assay was conducted.[18] Transient cotransfection of DLD-1 cells and RKO cells with the reporter plasmid and pre-*miR-128* significantly reduced luciferase activity as compared with the negative control ($P = 0.021$; Fig. 1b). These data suggested that *NEK2* mRNA was a direct functional target of *miR-128*. Using qRT-PCR, we confirmed that *miR-128* expression in cells transfected with pre-*miR-128* was significantly higher than that in cells transfected with the pre-*miR* negative control ($P < 0.05$; Fig. 1c). Then, cell lysates prepared from transfected cells were analyzed by qRT-PCR (Fig. 1d) and Western blot analysis (Fig. 1e) and we verified that *miR-128* suppressed *NEK2* in CRC cells.

MiR-128 Suppressed CRC Cell Proliferation by Inducing Cell Cycle Arrest

We hypothesized that *miR-128* could function as a tumor suppressor via the regulation of *NEK2* expression. To explain the antitumor efficacy of *miR-128* in CRC cells, proliferation assays were conducted in CRC cells transfected with pre-*miR-128* and negative control cells. *miR-128* suppressed the proliferation of both of these CRC cell lines (DLD-1, $P = 0.015$; RKO, $P = 0.013$; Fig. 2a).

FIG. 2 *MiR-128* inhibited cancer cell proliferation and was down-regulated by DNA methylation. **a** *MiR-128* inhibited the proliferation of the CRC cell lines DLD-1 (*left*) and RKO (*right*). Cells transfected with pre-*miR-128* or pre-*miR* negative control were seeded at 4.0×10^3 cells per well in 96-well plates and were analyzed by MTT assay. *Error bars* represent the SD from six replicates. **b** DLD-1 and RKO cells were transfected with *NEK2* specific siRNA (si*NEK2*) and negative control siRNA (siNC). Then, knockdown of *NEK2* was verified by qRT-PCR (*upper*) and Western blot analysis (*lower*) analyses. **c** Cells transfected with *NEK2* specific siRNA (si*NEK2*) or negative control siRNA (siNC) were seeded at 4.0×10^3 cells per well in 96-well plates and were analyzed by MTT assay. Error bars represent the SD from three replicates. **d** cell cycle assay in CRC cells transfected with pre-*miR-128* or pre-miR negative control. Cells were serum starved for 72 h to induce cell cycle arrest and were then cultured with serum for 24 h. *Error bars* represent the SD from three replicates. **e** CRC cell lines were cultured in the absence or presence of demethylating treatment with 5-aza for 48 h. *MiR-128* levels in 5-aza-treated cells were significantly higher than those in control cells. *Error bars* represent the SD from three replicates. **f** The DNA methylation status of CpG islands around *miR-128* in 4 CRC cell lines was analyzed by the quantification tool for methylation analysis (QUMA). **g** Cells were cultured in the absence or presence of demethylating treatment with 5-aza for 48 h. Relative *NEK2* mRNA levels in 5-aza-treated cells were significantly lower than those in control cells. *Error bars* represent the SD from three replicates

Next, to investigate whether the antitumor efficacy of *miR-128* was associated with the down-regulation of *NEK2* and cell cycle arrest, we investigated the impact of *NEK2* on CRC. Cell proliferation was inhibited by knock down of *NEK2* (Fig. 2b) in both cell lines (Fig. 2c). In addition, cell cycle analysis was conducted in pre-*miR-128*-transfected cells or negative control cells (DLD-1 and RKO cell lines). In cells transfected with pre-*miR-128*, an obvious increase in the number of cells at G_2 phase was observed. These data indicated that pre-*miR-128* induced G_2 arrest in CRC cells (Fig. 2d).

MiR-128 was Down-regulated by DNA Methylation in CRC Cells

Several reports have investigated the mechanisms through which *miR-128* is down-regulated in malignant tissues. Since Tsuruta et al.[19] reported that tumor suppressor microRNAs, including *miR-128*, are silenced by aberrant DNA hypermethylation, we investigated the mechanisms through which *miR-128* functioned in CRC cells, with an emphasis on epigenetics. First, to determine whether the expression of *miR-128* was silenced by DNA methylation, we examined the reactivation of *miR-128* expression in CRC cells and negative control cells by 5-aza-dCyd treatment. A two to threefold recovery of *miR-128* expression was found after 5-aza-dCyd treatment (Fig. 2e). Furthermore, bisulfite sequencing of the promoter region of *miR-128* in all 4 CRC cell lines verified the

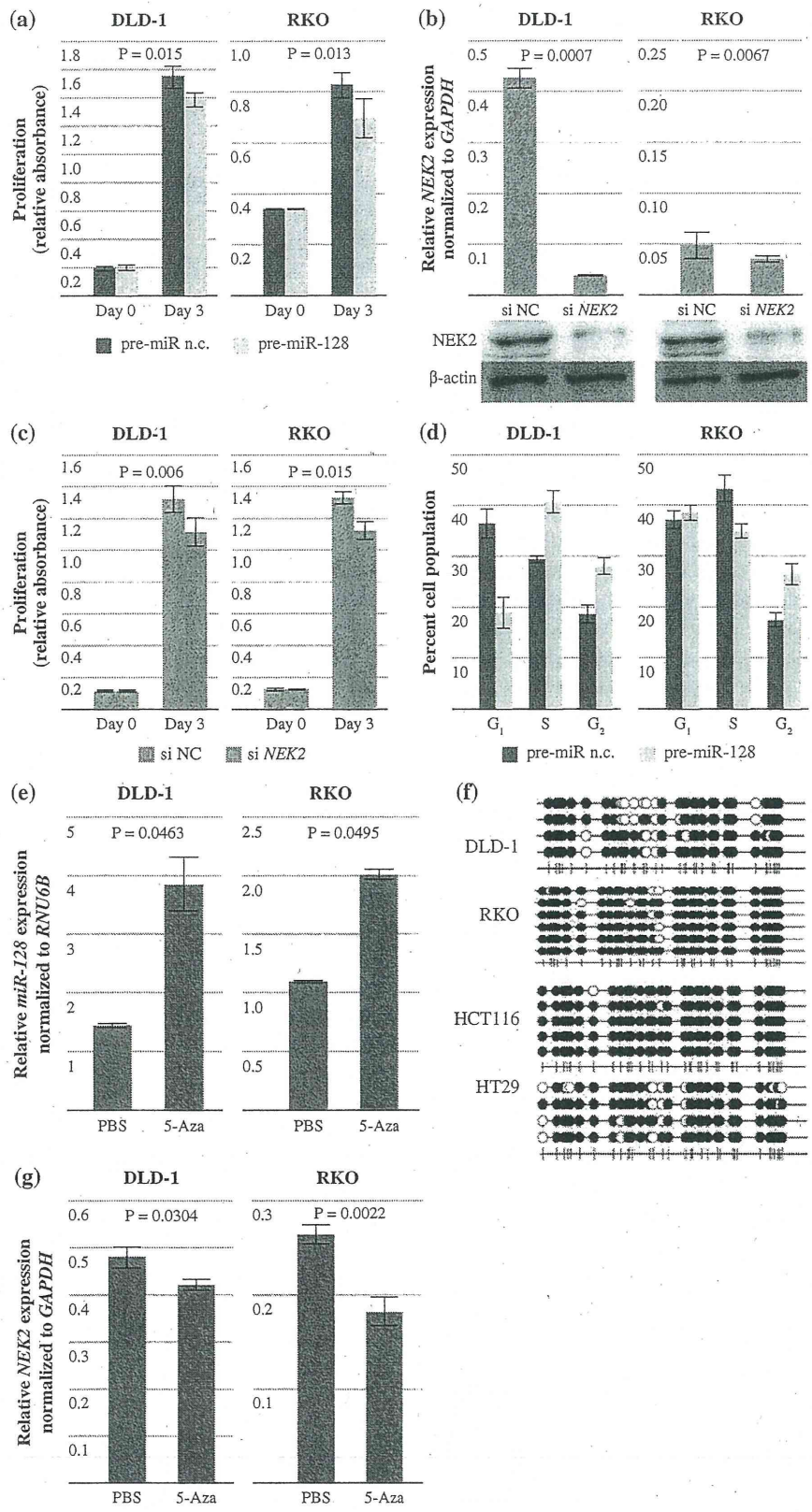
(a)
DLD-1
RKO
Proliferation (relative absorbance)
P = 0.015
P = 0.013
Day 0
Day 3
pre-miR n.c.
pre-miR-128
(b)
DLD-1
RKO
Relative NEK2 expression normalized to GAPDH
P = 0.0007
P = 0.0067
si NC
si NEK2
NEK2
β-actin
(c)
DLD-1
RKO
Proliferation (relative absorbance)
P = 0.006
P = 0.015
si NC
si NEK2
(d)
DLD-1
RKO
Percent cell population
G1
S
G2
pre-miR n.c.
pre-miR-128
(e)
DLD-1
RKO
Relative miR-128 expression normalized to RNU6B
P = 0.0463
P = 0.0495
PBS
5-Aza
(f)
DLD-1
RKO
HCT116
HT29
(g)
DLD-1
RKO
Relative NEK2 expression normalized to GAPDH
P = 0.0304
P = 0.0022
PBS
5-Aza

marked methylation of the promoter region of *miR-128* (Fig. 2f). In addition, *NEK2* expression levels were significantly reduced after 5-aza-dCyd treatment (Fig. 2g).

Clinicopathological Significance of and Inverse Relationship Between NEK2 and MiR-128 Expression

NEK2 mRNA expression in 180 tumor tissues and *miR-128* expression in 135 tumors from CRC patients were examined by qRT-PCR to investigate the clinical significance of *NEK2* and *miR-128* in CRC. We divided the 180 patients with CRC into a high *NEK2* expression group ($n = 90$) and a low *NEK2* expression group ($n = 90$), classified as having expression levels higher or lower than the median value, respectively. Clinicopathological factors were then analyzed in the high and low *NEK2* mRNA expression groups (Table 1). The high *NEK2* expression group showed greater tumor depth, lymphatic invasion, and peritoneal dissemination than the low *NEK2* mRNA expression group. With regard to overall survival, patients with high *NEK2* expression had a significantly poorer prognosis than those with low *NEK2* expression ($P = 0.0127$; Fig. 3a). Univariate and multivariate analysis showed that *NEK2* mRNA expression was an independent prognostic indicator of overall survival in patients with CRC (relative risk: 1.50, $P = 0.046$; Table 2).

Next, for *miR-128* expression analysis, we divided these 135 patients with CRC into a high *miR-128* expression group ($n = 67$) and a low *miR-128* expression group ($n = 68$), which were classified as having expression levels higher or lower than the median value, respectively. Clinicopathological factors and overall survival were then analyzed in the high and low *miR-128* expression groups, but no significant differences were observed between groups. With regard to disease-free survival (108 patients, excluding stage IV, were applied to this analysis), however, patients with low *miR-128* expression ($n = 54$) had a significantly poorer prognosis than those with high *miR-128* expression ($n = 55$; $P = 0.0149$; Fig. 3b). Moreover, as for the correlation between *NEK2* and *miR-128* expression, the high *miR-128* expression group exhibited significantly lower *NEK2* expression than the low *miR-128* expression group ($P = 0.007$; Fig. 3c). These results were consistent with data demonstrating that *miR-128* directly targeted the important independent prognostic indicator, *NEK2*.

TABLE 1 *NEK2* mRNA expression and clinicopathological factors in 180 colorectal cancer patients

Factor	Low expression ($n = 90$)		High expression ($n = 90$)		*P*
	n	%	*n*	%	
Age (years)					
<65	30	33.3	39	43.3	0.167
>66	60	66.7	51	56.7	
Sex					
Male	54	60	50	55.6	0.546
Female	36	40	40	44.4	
Histological grade					
Well-/moderately differentiated	84	93.3	82	91.1	0.787
Other	6	6.7	8	8.9	
Tumor size					
<30 mm	24	26.7	19	21.1	0.488
≥30 mm	66	73.3	71	78.9	
Serosal invasion					
Absent	35	38.9	21	23.3	<0.001*
Present	55	61.1	69	76.7	
Lymph node metastasis					
N0	58	64.4	39	43.3	0.070
N1–2	32	35.6	51	56.7	
Lymphatic invasion					
Absent	62	31.1	46	51.1	<0.001*
Present	28	68.9	44	48.9	
Venous invasion					
Absent	75	83.3	71	78.9	0.446
Present	15	16.7	19	21.1	
Liver metastasis					
Absent	82	91.1	82	91.1	1
Present	8	8.9	8	8.9	
Peritoneal dissemination					
Absent	90	100	84	93.3	0.004*
Present	0	0	6	6.7	
Distant metastasis					
Absent	89	98.9	87	96.7	0.650
Present	1	1.1	3	3.3	
AJCC stage					
0, I, II	54	60	39	43.3	0.025*
III, IV	36	40	51	56.7	

Well well-differentiated adenocarcinoma, *Moderately* moderately differentiated adenocarcinoma, *Others* poorly differentiated adenocarcinoma and mucinous carcinoma, *AJCC* American Joint Committee on Cancer

* $P < 0.05$

DISCUSSION

In this study, we found that high *NEK2* expression in CRC tissues was associated with a poor prognosis. Several previous studies have supported these results and provided insights into the molecular mechanisms involved. For example, Suzuki et al.[11] reported that transfection with *NEK2* siRNA resulted in the inhibition of cell proliferation, induction of apoptosis in vitro, and suppression of tumor